ATTACHMENT 6

AREVA NP Inc. Affidavit and Non-Proprietary Version of Attachment 3

AFFIDAVIT

COMMONWEALTH OF VIRGINIA)
) ss.
CITY OF LYNCHBURG)

1. My name is Gayle F. Elliott. I am Manager, Product Licensing, for AREVA NP Inc. and as such I am authorized to execute this Affidavit.

2. I am familiar with the criteria applied by AREVA NP to determine whether certain AREVA NP information is proprietary. I am familiar with the policies established by AREVA NP to ensure the proper application of these criteria.

3. I am familiar with the AREVA NP information contained in the report ANP-2843(P), Revision 1, entitled "LaSalle Unit 2 Nuclear Power Station Spent Fuel Storage Pool Criticality Safety Analysis with Neutron Absorbing Inserts and Without Boraflex," dated August 2009 and referred to herein as "Document." Information contained in this Document has been classified by AREVA NP as proprietary in accordance with the policies established by AREVA NP for the control and protection of proprietary and confidential information.

4. This Document contains information of a proprietary and confidential nature and is of the type customarily held in confidence by AREVA NP and not made available to the public. Based on my experience, I am aware that other companies regard information of the kind contained in this Document as proprietary and confidential.

5. This Document has been made available to the U.S. Nuclear Regulatory Commission in confidence with the request that the information contained in this Document be withheld from public disclosure. The request for withholding of proprietary information is made in

accordance with 10 CFR 2.390. The information for which withholding from disclosure is requested qualifies under 10 CFR 2.390(a)(4) "Trade secrets and commercial or financial information."

6. The following criteria are customarily applied by AREVA NP to determine whether information should be classified as proprietary:

(a) The information reveals details of AREVA NP's research and development plans and programs or their results.

(b) Use of the information by a competitor would permit the competitor to significantly reduce its expenditures, in time or resources, to design, produce, or market a similar product or service.

(c) The information includes test data or analytical techniques concerning a process, methodology, or component, the application of which results in a competitive advantage for AREVA NP.

(d) The information reveals certain distinguishing aspects of a process, methodology, or component, the exclusive use of which provides a competitive advantage for AREVA NP in product optimization or marketability.

(e) The information is vital to a competitive advantage held by AREVA NP, would be helpful to competitors to AREVA NP, and would likely cause substantial harm to the competitive position of AREVA NP.

The information in the Document is considered proprietary for the reasons set forth in paragraphs 6(b) and 6(c) above.

7. In accordance with AREVA NP's policies governing the protection and control of information, proprietary information contained in this Document have been made available, on a limited basis, to others outside AREVA NP only as required and under suitable agreement providing for nondisclosure and limited use of the information.

8. AREVA NP policy requires that proprietary information be kept in a secured file or area and distributed on a need-to-know basis.

9. The foregoing statements are true and correct to the best of my knowledge, information, and belief.

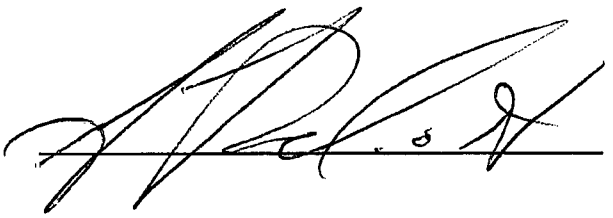

SUBSCRIBED before me this 11th day of August 2009.

Sherry L. McFaden
NOTARY PUBLIC, COMMONWEALTH OF VIRGINIA
MY COMMISSION EXPIRES: 10/31/10
Reg. # 7079129

SHERRY L. MCFADEN
Notary Public
Commonwealth of Virginia
7079129
My Commission Expires Oct 31, 2010

An AREVA and Siemens company

ANP-2843(NP)
Revision 1

LaSalle Unit 2 Nuclear Power Station Spent Fuel Storage Pool Criticality Safety Analysis with Neutron Absorbing Inserts and Without Boraflex

August 2009

AREVA NP Inc.

ANP-2843(NP)
Revision 1

LaSalle Unit 2 Nuclear Power Station Spent Fuel Storage Pool Criticality Safety Analysis with Neutron Absorbing Inserts and Without Boraflex

sjp

AREVA NP Inc.

ANP-2843(NP)
Revision 1

Nature of Changes

Item	Page	Description and Justification
1	2-4	Punctuation corrected
2	2-5	4 °C added for clarification
3	4-4,6-13	Proprietary markings removed from insert parameters
4	5-1	Space added

Contents

Tables

Figures

Nomenclature

BAF	bottom of active fuel
BOL	beginning of life
BWR	boiling-water reactor
CPR	critical power ratio
CW	clock-wise
EALF	the energy of the average lethargy causing fission
GWd	energy unit, giga-watt-day
k-eff	effective neutron multiplication factor
k_∞	infinite lattice neutron multiplication factor
LHGR	linear heat generation rate
PLR	part-length fuel rod
NRC	Nuclear Regulatory Commission, U. S.
REBOL	reactivity-equivalent at beginning of life (fresh fuel, no Gd_2O_3, no fission products)
TD	theoretical density
H/X	atomic ratio of hydrogen (H) to fissile isotopes (X)

1.0 Introduction

This report presents the results of a criticality safety evaluation performed for the LaSalle Unit 2 Nuclear Power Station spent fuel storage pool assuming complete Boraflex degradation and the use of neutron absorbing inserts in each accessible storage cell. Reference 1 is the last criticality safety evaluation that was submitted for NRC review for the LaSalle Unit 2 spent fuel pool.

In this report, a reference bounding assembly has been defined to bound the reactivity of all past and current fuel assembly types delivered to the LaSalle station (both Units 1 and 2). This reference bounding assembly is based on an AREVA NP Inc.* ATRIUM†-10 fuel assembly. This analysis demonstrates that with the reference bounding assembly, complete Boraflex degradation, and a neutron absorbing NETCO-SNAP-IN insert in each storage cell, the pool k-eff remains below the 0.95 k-eff acceptance criterion established by the NRC.

* AREVA NP Inc. is an AREVA and Siemens company.

† ATRIUM is a trademark of AREVA NP.

2.0 Summary

Criticality analyses have been performed and are documented herein for the LaSalle Unit 2 spent fuel pool assuming no Boraflex and the presence of a NETCO-SNAP-IN insert in each accessible storage cell of the rack. The criticality analyses are based on the use of a reference fuel assembly design that is bounding of (i.e., more reactive than) all fuel designs used in Units 1 and 2 at the LaSalle station. The KENO V.a code was used for all calculations that do not require fuel depletion. The CASMO-4 code is used to compare lattice k_∞ values at peak reactivity conditions and in defining the gadolinia manufacturing uncertainty. Benchmarking is included for both the KENO V.a and CASMO-4 codes.

The calculations documented herein demonstrate that the ATRIUM-10 reference bounding assembly design has been selected to be more reactive, in an in-rack configuration without Boraflex and with the NETCO-SNAP-IN inserts, than any of the current or past fuel assembly designs used in the LaSalle reactors. These comparisons are based upon actual GE 8x8, ATRIUM-9, GE14, ATRIUM 10XM and ATRIUM-10 lattice geometries and enrichment distributions and the results are shown in Appendix B. This evaluation establishes that the fuel assemblies previously manufactured for use in the LaSalle reactors can be safely stored in the LaSalle Unit 2 spent fuel storage pool with NETCO-SNAP-IN inserts.

The reference bounding assembly is defined with two U235 enrichment / gadolinia concentration zones. The bottom enrichment / gadolinia zone is divided into two separate axial zones by the ATRIUM-10 geometry transition at 96". This creates the 3 zones shown in Figure 2.1. Three REBOL lattices have been defined to represent the lattices of the reference bounding assembly in KENO calculations. The reactivity of the REBOL lattices have been increased to compensate for the uncertainties associated with defining these maximum reactivity lattices.

This evaluation includes manufacturing uncertainties for the ATRIUM-10 fuel design and the fuel pool storage racks, code modeling uncertainties, reactivity increases due to accident or abnormal conditions, and one-sided tolerance multipliers to determine the 95/95 upper limit k-eff. The conditions and uncertainties assumed in this analysis are described in Section 6.

This evaluation demonstrates that the reference ATRIUM-10 fuel assembly does not exceed an array k-eff of 0.95 in the LaSalle Unit 2 spent fuel storage pool without Boraflex, provided the

neutron absorbing insert depicted in Figure 4.2 has been installed in each accessible storage cell. As defined in Table 2.1, ATRIUM-10 fuel that contains equivalent or less enrichment and equivalent or higher Gd_2O_3 concentrations in the fuel zones depicted in Figure 2.1 can be safely stored in the LaSalle Unit 2 spent fuel storage pool. In addition, ATRIUM-10 fuel that contains more enrichment and/or lower Gd_2O_3 concentrations than the reference assembly design can be safely stored provided each zone of the assembly is less reactive than the corresponding zone of the reference assembly design. This can be established using the storage rack model in the CASMO-4 lattice physics code as described in Appendix A.

This analysis considers unchanneled fuel assemblies as well as assemblies with the AREVA 100 mil fuel channel.* Additionally, there is no limitation for bundle orientation or position in the storage cell since these are accounted for in the analysis.

To assure that the actual reactivity will always be less than the calculated reactivity, the following conservative assumptions have been made:

- The results are based on a moderator temperature of 4°C (39.2°F), which gives the highest reactivity for the fuel storage pool for a configuration assuming no Boraflex with NETCO-SNAP-IN inserts.
- Fuel assemblies are assumed to contain the high reactivity reference bounding lattices for the entire length of the assembly, (natural uranium blankets are not modeled).
- Each lattice in each fuel assembly in the array is assumed to be at its lifetime maximum reactivity level, (no credit is taken for assembly burnup).
- The most limiting orientation or position of each assembly in its rack cell is accounted for in the analysis.
- The analysis takes into account storage with or without fuel channels. (The array k-eff is higher with a fuel channel present).
- Neutron absorption in fuel assembly structural components (spacers†, tie plates, etc) is neglected.‡
- The maximum reactivity value includes all significant manufacturing and calculational uncertainties.

---

* The AREVA advanced fuel channel and the AREVA 80 mil fuel channel are also acceptable.

† It is conservative to neglect the spacers because this spent fuel pool contains no soluble boron and the region around the fuel rods is under-moderated and neglecting the spacer places more water within the calculational model. In addition, the inconel springs are a stronger neutron absorber than water.

‡ The active fuel region repeats periodically in the vertical direction. Therefore, neutron absorption in upper and lower tie plates, fuel plenums, etc. is neglected.

- The reactivity of the REBOL lattices used in the KENO analysis have been designed to be at least 0.010 Δk more reactive than the reference bounding lattices they represent. This is more than the uncertainty associated with defining these maximum reactivity lattices.

Table 2.1 Criticality Safety Limitations for ATRIUM-10 Fuel Assemblies Stored in the LaSalle Unit 2 Nuclear Power Station Spent Fuel Pool

1. ATRIUM-10 Fuel Configuration

Parameter	Nominal ATRIUM-10 Value
Clad OD, in.	0.3957
Clad ID, in.	0.3480
Pellet Diameter, in.	0.3413
Rod Pitch, in.	0.510
Fuel Density % Theoretical	95.85 to 96.26
Water Rods	Internal Channel

2. Fuel may be stored with or without fuel channels.

3. Fuel Design Limitations for Enriched Lattices*

The U235 enrichment and gadolinia concentration levels must meet the requirements specified below and shown graphically in Figure 2.1 (dimensions represent fuel column height above BAF).

Above 126"	Maximum Lattice Average Enrichment, wt% U-235	4.47
	Minimum Number of Rods containing Gd_2O_3	10
	Minimum wt% Gd_2O_3 in each Gd Rod	3.5

Below 126" †	Maximum Lattice Average Enrichment, wt% U-235	4.57
	Minimum Number of Rods containing Gd_2O_3	10
	Minimum wt% Gd_2O_3 in each Gd Rod	6.0

Eight gadolinia rods must be loaded one row in from the edge of the lattice such that rows 2 and 9 and columns 2 and 9 each contain 2 gadolinia rods.

4. ATRIUM-10 fuel assemblies which do not meet the limitations above may be stored in the LaSalle Unit 2 spent fuel pool provided the reactivity of any enriched lattice does not exceed the following in-rack k_∞ values at any point during their lifetime. (The CASMO-4 storage rack model that must be used for this calculation is defined in Appendix A and the

* These are the reference bounding lattices described on Page 6-2.

† This is actually two axial zones divided by the geometry of the ATRIUM-10 part-length rod transition at 96" above BAF.

transition between top and bottom lattice geometries occurs at 96 inches from the bottom of the fueled length.)

Zone	Lattice Geometry	Distance from BAF	Max. in-rack k_∞ (4°C)
3	A10T (83 rods)	126" to 149"	0.9185
2	A10T (83 rods)	96" to 126"	0.8869
1	A10B (91 rods)	0" to 96"	0.8843

5. The spent fuel storage rack design parameters and dimensions are as defined in Reference 4, and a general description of the NETCO-SNAP-IN inserts is provided in Reference 5.

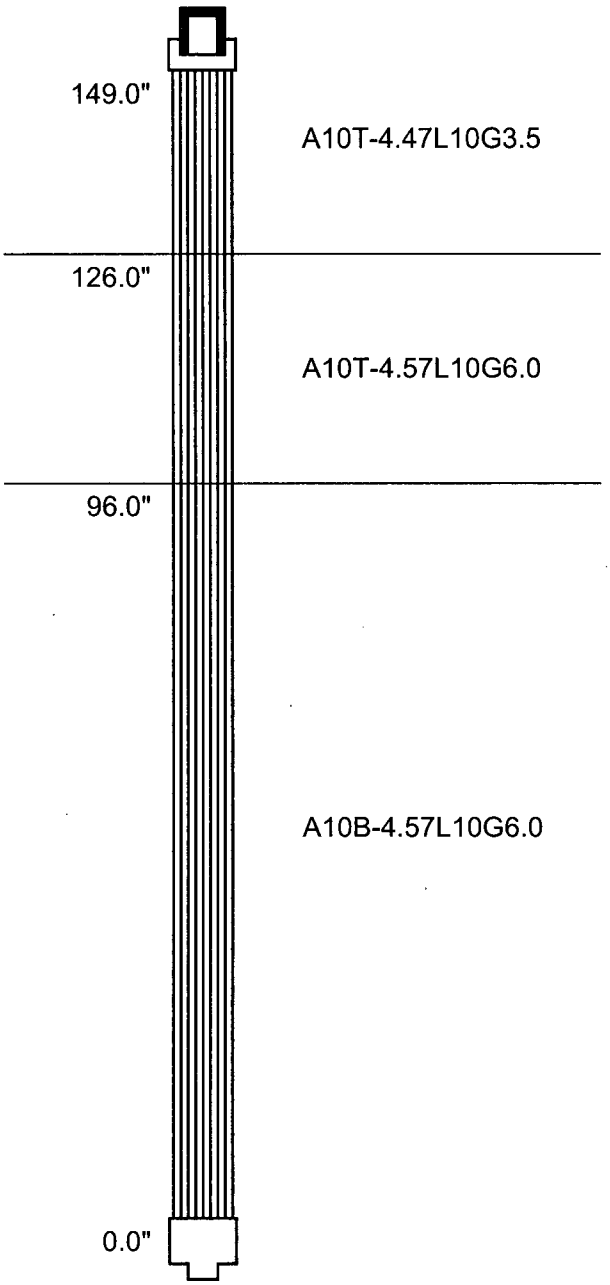

Figure 2.1 ATRIUM-10 Reference Bounding Assembly

3.0 Criticality Safety Design Criteria

The criticality safety design criteria defined in the following documents are applicable for this LaSalle Unit 2 Nuclear Power Station spent fuel storage facility evaluation:

A. Subsection B.4 of 10CFR 50.68, (Criticality Accident Requirements), (Reference 6).

B. Section 9.1.1 (Fresh and Spent Fuel Storage and Handling) of the Standard Review Plan (Reference 7).

C. ANSI/ANS American National Standard 57.2-1983 (*Design Requirements for Light Water Reactor Spent Fuel Storage Facilities at Nuclear Power Plants*) issued by the American Nuclear Society (Reference 8).*

D. ANSI/ANS American National Standard 8.17-1984 (*Criticality Safety Criteria for the Handling, Storage and Transportation of LWR Fuel Outside Reactors*) issued by the American Nuclear Society, January 1984 (Reference 9).

E. "OT Position for the Review and Acceptance of Spent Fuel Storage and Handling Applications," issued by the NRC in 1978 and amended in 1979 (Reference 10).

F. "Guidance on the Regulatory Requirements for Criticality Analysis of Fuel Storage at Light-Water Reactor Power Plants," issued by the NRC in 1998 (Reference 11).

These documents define the assumptions and acceptance criteria used in this evaluation. In descending order (from A to F), these documents go from "least" to "most" detail relative to explicitly defining what needs to be addressed in the criticality safety evaluation. In general, the criticality safety acceptance criterion applicable to this evaluation is as defined by Section 9.1.1 of the Standard Review Plan (Reference 7):

> ...the k-eff will not exceed 0.95 for all normal and credible abnormal conditions.

This is consistent with requirements in the LaSalle FSAR and Technical Specifications.

---

* ANSI/ANS 57.1 and 57.3 are endorsed in combination with ANSI/ANS 57.2 in item B. ANSI/ANS 57.1 and 57.3 are not cited here because they do not apply to spent fuel pool criticality.

4.0 Fuel and Storage Array Description

LaSalle Units 1 and 2 have loaded four different product lines—GE 8x8 fuel, ATRIUM-9 fuel, GE14 fuel, and ATRIUM-10 fuel. The ATRIUM-10 fuel product line is the fuel currently being loaded in reload quantities in both LaSalle reactors. All four of these designs are stored in the LaSalle Unit 2 spent fuel storage pool. In an in-rack configuration assuming no Boraflex and NETCO-SNAP-IN inserts, the reference ATRIUM-10 design has a higher reactivity than all previously loaded fuel assembly designs. Appendix B provides information from which this conclusion can be made. As such, the ATRIUM-10 reference bounding assembly design forms the basis for demonstrating that the maximum k-eff of the spent fuel pool storage array without Boraflex with NETCO-SNAP-IN inserts remains less than 0.95.

4.1 *Fuel Assembly Design*

The ATRIUM-10 fuel assembly is a 10x10 fuel rod array with an internal square water channel offset in the center of the assembly (taking the place of nine fuel rod locations). The assembly contains part-length fuel rods (PLR); therefore, a "top" lattice geometry will apply above the PLR boundary and a "bottom" lattice geometry will apply below the PLR boundary. The ATRIUM-10 mechanical design parameters are summarized in Table 4.1. A representation of the ATRIUM-10 assembly design is depicted in Figure 4.1. The ATRIUM-10 fuel in the LaSalle Nuclear Power Station has used and will use the standard 100 mil fuel channel design.

4.2 *Fuel Storage Racks*

The spent fuel storage rack dimensions and details are shown in Reference 4. The key rack assembly dimensions and tolerances are listed in Table 4.2. The fuel pool storage cell with ATRIUM-10 fuel has been modeled in CASMO-4 as shown in Figure 4.2 with small variations in KENO V.a. Each rack consists of an array of stainless steel boxes with a separation of 0.075" between each box wall. Originally this separation was filled with a layer of Boraflex material; however, for this analysis it is assumed that the Boraflex has been removed and is now replaced with water.

For this evaluation, a chevron shaped neutron absorbing insert (NETCO-SNAP-IN) is modeled in each of the storage cells (see the general description in Reference 5). These inserts will extend over the full length of the fueled zone and will maintain the same orientation in each

storage cell. Based on the insert configuration of Figure 4.3, peripheral storage cells on the north and east sides of the storage pool will not be completely surrounded by four wings of the absorbing insert. In the actual Unit 2 pool configuration, there will also be a minimal number of peripheral cells on all sides of the storage pool that will not be completely surrounded by four wings of the absorbing insert due to geometric layout and inaccessible storage locations.

Table 4.1 ATRIUM-10 Fuel Assembly Parameters

Fuel Assembly	
Fuel Rod Array	10x10
Fuel Rod Pitch, in.	0.510
Number of Fuel Rods Per Assembly	91
Water Channel	1
Fuel Rods	
Fuel Material	UO_2
Pellet Density, % of Theoretical	96.26*
Pellet Diameter, in.	0.3413
Pellet Void Volume, %	
Enriched UO_2	1.2†
Cladding Material	Zircaloy-2
Cladding OD, in.	0.3957
Cladding ID, in.	0.3480
Internal Water Channel	
Outside Dimension, in.	1.378
Inside Dimension, in.	1.321
Channel Material	Zircaloy 2 or Zircaloy-4
Fuel Channel (standard 100 mil)‡	
Outside Dimension, in.	5.478
Inside Dimension, in.	5.278
Channel Material	Zircaloy-2, Zircaloy-4, or Zirc-BWR
Fuel Column Lengths	
Distance from the bottom of the fuel to the top of the fuel in the part length fuel rods, in.	96.0
Total Fueled Length, in.	149.0

* Criticality safety analysis is valid for nominal pellet densities between 95.85% and 96.26% TD.

† Depending on pellet L/D, the pellet void volume can vary. A nominal value of 1.2% was assumed for the criticality safety analysis. Variations of the void volume are not significant relative to impact on storage array criticality safety. (Use of chamfered pellets with higher void volumes are also acceptable)

‡ The conclusions in this report are equally valid for fuel channels that may differ. Hence, conclusions remain valid for other fuel channel types, e.g., advanced channels etc. (See discussion about fuel channels in Section 6.2).

Table 4.2 Fuel Storage Rack Parameters

Parameter	Value
Insert, B-10 areal density, g/cm^2	0.0086 minimum
Insert wing thickness, in.	0.065 ± 0.005
Material	Aluminum and B-10
Insert modeled wing length, in.	5.98*
Storage cell Inside Dimension, in.	6.00 ± 0.02
Inner rack box wall thickness, in.	0.090 ± 0.009
Box material	Stainless steel
Original Boraflex thickness, in.	0.075 ± 0.007
Material	Originally Boraflex, now modeled as water
Nominal rack cell pitch, in.	6.255 [ ]

* Value used in the KENO model. 6.00" was used in the CASMO-4 model which requires the insert wing to extend to the inside wall of the fuel storage cell.

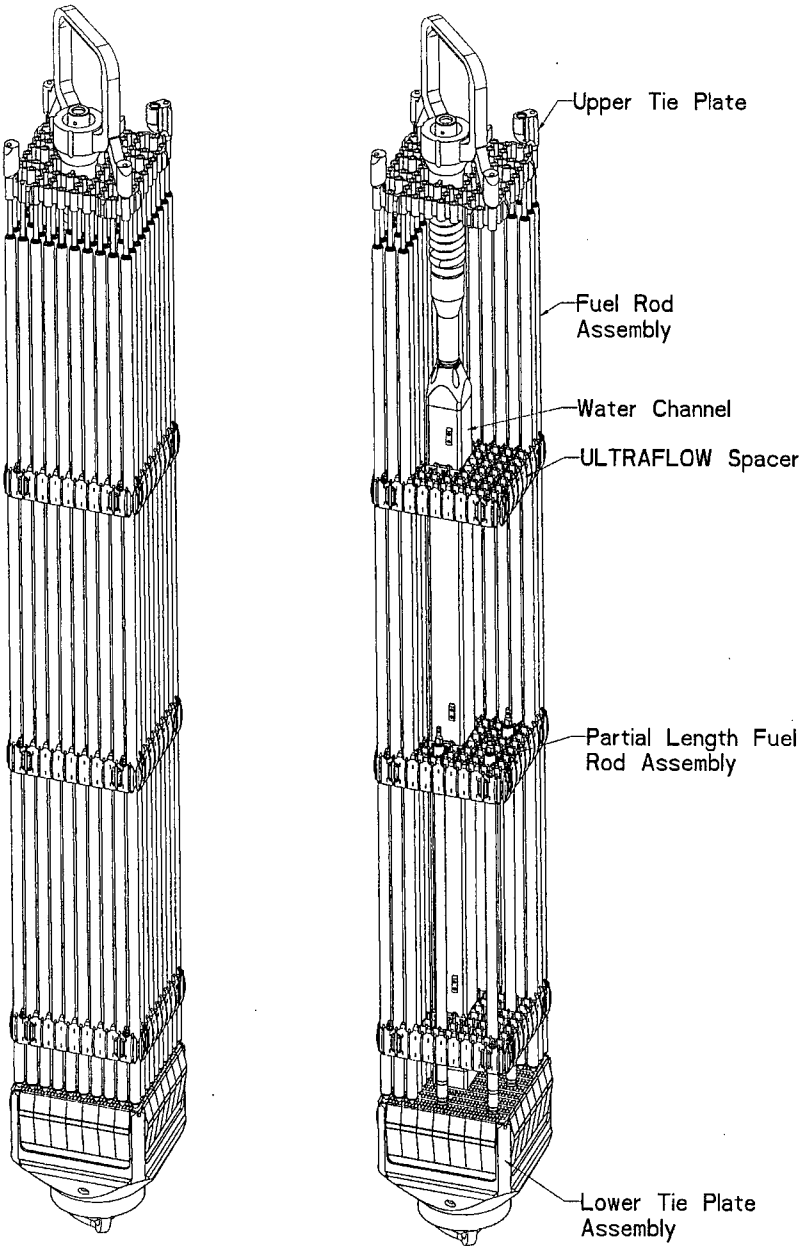

Figure 4.1 Representative ATRIUM-10 Fuel Assembly

(Assembly length and number of spacers has been reduced for pictorial clarity.)

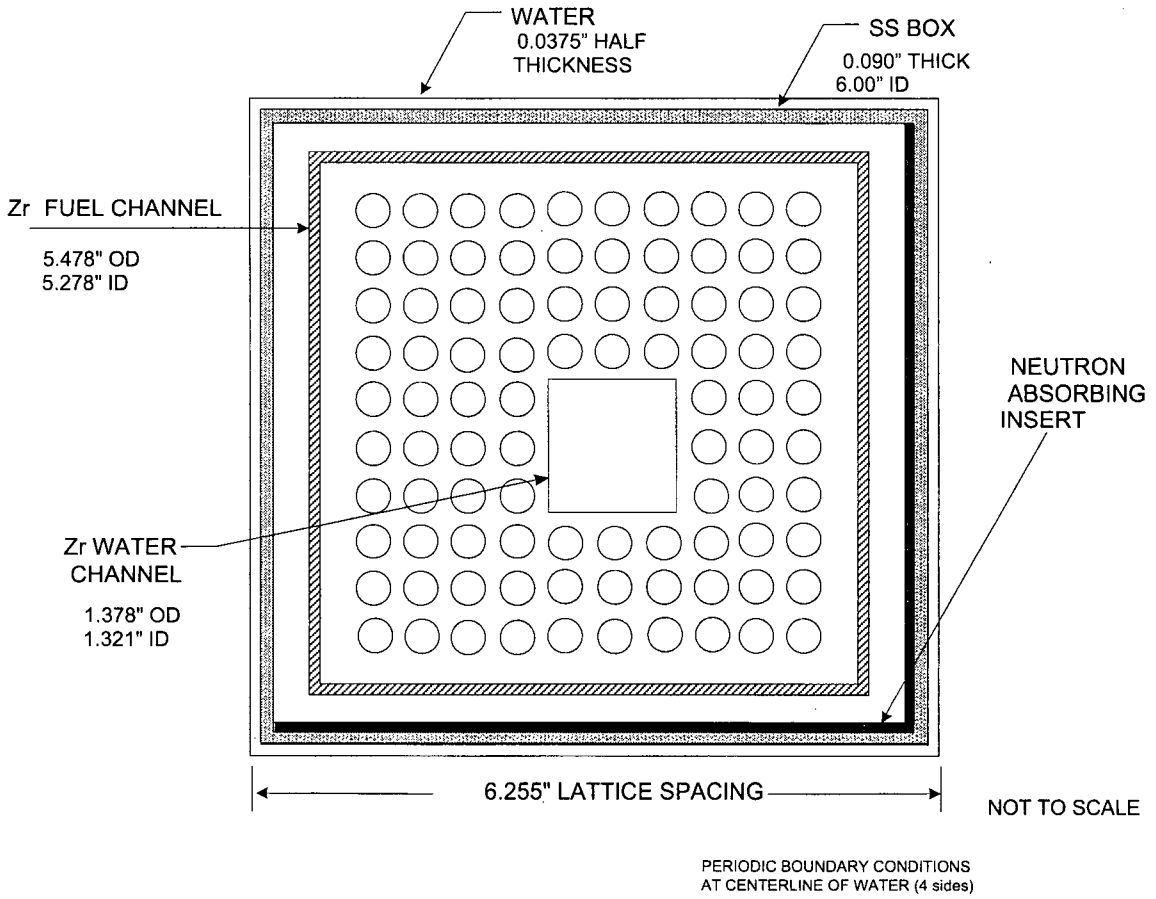

Figure 4.2 Calculational Model of Storage Cell

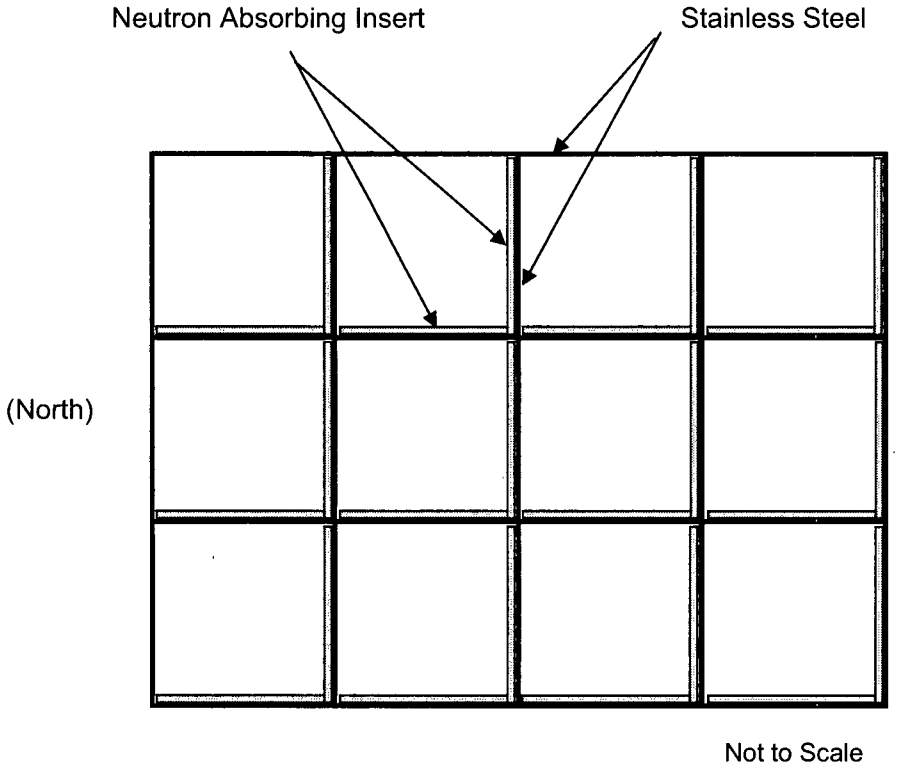

Figure 4.3 Storage Rack with Inserts

5.0 Calculation Methodology

The spent fuel storage criticality safety evaluation is performed with the KENO V.a Monte Carlo code, which is part of the SCALE 4.4a Modular Code System (Reference 2). The ENDF/B-V, 44 energy group data library is used by the SCALE driver module CSAS25, which uses modules BONAMI-2 and NITAWL to perform spatial and energy self-shielding adjustments of the cross sections for use in KENO V.a. AREVA has benchmarked KENO V.a in accordance with NUREG/CR-6698 (Reference 3) using critical experiments related to the storage of fuel assemblies in water - including neutron absorbing materials such as stainless steel and BORAL. For applications using the 44 energy group data libraries, the KENO V.a bias and standard deviation are 0.00542 and 0.00511, respectively (see Appendix C).

KENO V.a is run on the AREVA NP scientific computer cluster using the Linux operating system. The hardware and software configurations are governed by AREVA NP procedures to ensure calculational consistency in licensing applications. The code modules are installed on the system and the installation check cases are run to ensure the results are consistent with the installation check cases that are provided with the code. The binary executables are put under configuration control so that any changes in the software will require re-certification. The hardware configuration of each machine in the cluster is documented so that any significant change in hardware or operating system that could result in a change in results is controlled. In the event of such a change in hardware or operating system, the hardware validation suite is rerun to confirm that the system still performs as it did when the code certification was performed.

In this analysis the SCALE 4.4a code system is employed to:

- Calculate Dancoff coefficients
- Calculate absolute k-effective results for the LaSalle Unit 2 spent fuel pool
- Evaluate accident conditions, alternate loading conditions, and manufacturing tolerance conditions

The CASMO-4 code is used when conditions require fuel and gadolinia depletion. CASMO-4 is a multigroup, two-dimensional transport theory code with an in-rack geometry option where typical storage rack geometries can be defined on an infinite lattice basis. This code is used for fuel depletion and relative reactivity comparisons in a manner that is consistent with AREVA's

NRC approved CASMO-4 / MICROBURN-B2 methodology (Reference 12). CASMO-4 has been approved at LaSalle for BWR calculations and is included as a methodology reference (via Reference 12) in Section 5.6.5.B of the LaSalle Technical Specifications. The CASMO-4 computer code is controlled by AREVA procedures and the version used in this analysis meets the requirements of Reference 12.

In this analysis CASMO-4 is employed to:

- Perform in-core isotopic depletion at [ ] void history levels for fuel lattices.
- Perform in-rack k_∞ assessments to identify the lattices with maximum reactivity.
- Define lattices for a reference bounding assembly that represent the maximum reactivity condition supported by the analysis.
- Define the reactivity equivalent, beginning-of-life (REBOL) lattices with fresh fuel and no gadolinia, for the subsequent KENO V.a base case criticality calculations. Note that for the REBOL lattices, the U-235 content is manually adjusted upward until the REBOL k_∞ is at least 0.01 Δk greater than the lattices of the reference bounding assembly. This 0.01 Δk is used to account for calculational and depletion uncertainties of the CASMO-4 code as discussed in Appendix D.
- Evaluation of the manufacturing uncertainty for gadolinia content. This is needed since a lower gadolinia concentration will deviate from the nominal case more near peak reactivity than it will at beginning of life (i.e., in a REBOL assembly).

5.1 Area of Applicability

Table C.6 in Appendix C shows the ranges of key parameters represented in the KENO V.a benchmark analysis. Parameters such as rectangular lattices of zircaloy clad UO2 fuel rods in a pool of water with stainless steel and boron are sufficiently general to not require comparison. The remaining parameters are compared in the following table and show that the KENO V.a portion of this analysis has been performed within the range of experimental conditions used in the KENO V.a benchmark.

Parameter	Benchmark Values	Values in this Analysis
Enrichment (wt% U-235)	2.46 to 9.83	2.66 to 4.57
Pitch (cm)	1.04 to 2.64	1.27 to 1.31
H/X ratio	17.4 to 473	250 to 350
Energy of the Average Lethargy Causing Fission (eV)	0.11 to 2.51	0.19 to 0.26

For the CASMO-4 qualification, ATRIUM-10 fuel lattices were modeled using the LaSalle fuel storage rack geometry. Therefore, the CASMO-4 calculations performed for this evaluation are within the area of applicability of the comparisons shown in Appendix D.

6.0 Criticality Safety Analysis

The criticality safety evaluation uses a reference bounding assembly comprised of two top and one bottom geometry reference bounding lattices* to demonstrate that the upper limit $k_{95/95}$ k-eff for the LaSalle Unit 2 Nuclear Power Station spent fuel pool can be met. These evaluations include the worst credible conditions and uncertainties as defined in the references documented in Section 3.0. The reference bounding ATRIUM-10 bundle is comprised of three axial zones each with ten gadolinia rods. These zones are described in the following table and are shown graphically in Figure 2.1.

Zone	Lattice Geometry	Distance from BAF	U235 wt%	Gadolinia wt%
3	A10T	126" to 149"	4.47	3.5
2	A10T	96" to 126"	4.57	6.0
1	A10B	0" to 96"	4.57	6.0

6.1 *Geometry Model*

The ATRIUM-10 fuel assembly parameters are given in Table 4.1. The key fuel pool storage rack parameters are given in Table 4.2. The main KENO storage rack geometry model used for analysis is an infinite array of stainless steel fuel storage boxes with a chevron shaped neutron absorbing insert in each accessible box. All inserts will have the same orientation throughout the entire spent fuel pool; therefore, the fuel assemblies loaded on 2 sides of the perimeter will not be completely enclosed by the inserts (see Figure 4.3). All accessible storage rack cells are modeled with an ATRIUM-10 fuel assembly.

6.2 *Definition of REBOL Lattices*

The CASMO-4 lattice depletion calculations are performed at hot operating, uncontrolled, [ ] void history conditions[†]. The calculation results are based upon the nominal fuel design parameters (defined in Table 4.1) and assume a standard 100 mil fuel channel. Cold xenon-free restart calculations are performed as a function of exposure and void history to establish the highest in-rack reactivity (k_∞) at any time throughout the life of the fuel lattice. The maximum CASMO-4 in-rack k_∞ of the reference bounding lattices are 0.8843, 0.8869, and

---

* It is demonstrated in Appendix B that the ATRIUM-10 reference design in the spent fuel pool geometry without Boraflex and with NETCO-SNAP-IN inserts is more reactive than the other fuel types used in the LaSalle reactors.

† [ ].

0.9185, for Zones 1 though 3 respectively. These limiting results are based upon a water temperature of 4 °C, 40% void history, and lattice exposures of 16.5, 16.0, and 11.5 GWd/MTU, respectively for each axial zone. The results of the CASMO-4 comparison calculations are summarized in Table 6.1.

The following table is provided to summarize the differences between the fuel assembly and lattice names used in this evaluation.

Fuel Lattice Type	Description
ATRIUM-10 REBOL Lattices (top and bottom zone geometries)	Defined for use in the KENO calculations, 2.66 wt% U235 (Zone 1), 2.72 wt% (Zone 2), and 3.05 wt% U235 (Zone 3), no gadolinia, uniform enrichment distribution, selected to be at least 0.01 Δk more reactive than the reference bounding lattices.
ATRIUM-10 Reference Bounding Lattices (top and bottom zone geometries)	The most reactive lattices supported by this evaluation with distributed enrichment distribution, 4.57 wt% U235 with 10 Gd_2O_3 rods at 6.0 wt% gadolinia (Zones 1 and 2), and 4.47 wt% U235 with 10 Gd_2O_3 rods at 3.5 wt% gadolinia in Zone 3. These lattices are defined to establish the minimum reactivity required for the REBOL lattices.
As-Fabricated Assemblies (ATRIUM-10, ATRIUM-9, GE14, and GE 8x8)	The actual assemblies built for and/or used in the LaSalle reactors. CASMO-4 in-rack k_∞ comparisons are included in Appendix B.

In support of the KENO rack calculations, reactivity equivalent beginning of life (REBOL) lattice enrichments are selected using the top and bottom ATRIUM-10 lattice geometries. Two REBOL lattices are created with the ATRIUM-10 top geometry and one with the ATRIUM-10 bottom geometry. The REBOL lattices have the same enrichment in all rods and no gadolinia. The REBOL lattice enrichments as well as the CASMO-4 in-rack k_∞ at 4°C are shown in Table 6.1.

As discussed in the methodology section, a 0.01 Δk adder is included in the generation of the REBOL lattices to address CASMO-4 code, geometry, material, and depletion uncertainties.

6.3 *Storage Array Reactivity*

For the general KENO rack array calculations, an infinite array of fuel storage cells was assumed – using periodic boundary conditions in all three directions. All fuel locations in the rack array model contain an ATRIUM-10 REBOL assembly comprised of a 3.05 wt% U-235 top zone (above 126"), a 2.72 wt% U-235 intermediate zone (96" to 126"), and a 2.66 wt% U-235 bottom zone (below 96"). The array k-eff is highest when the assembly is centered in the available water space in the storage cell and the assembly orientation shown in Figure 4.2 is as limiting as the other 3 simple rotation possibilities. Calculations were performed at temperatures of 4 °C, 20 °C, 100 °C and 120 °C*. As shown in Table 6.2, the limiting base case KENO k-eff is 0.916.

The KENO model assumes a standard 100 mil fuel channel. The array k-eff is about 0.006 Δk lower when the fuel channels are removed.† There is no significant difference in array reactivity between the AREVA standard 100 mil fuel channel and the AREVA advanced fuel channel.‡

As discussed in Section 4.2 and illustrated in Figure 4.3, assemblies loaded in storage cells on the top and left hand sides of the figure will not be completely surrounded by neutron absorbing inserts. (The entire spent fuel pool is shown in Figure 1.1 of Reference 1 and contains irregular regions). Since the main KENO calculations used an infinite 3-D model it is necessary to evaluate whether the lack of neutron absorbing inserts on these 2 edges of the pool will have a non-conservative effect. This was evaluated using finite 3-D KENO calculations with a 24x24 array of storage cells surrounded by water and concrete, (each cell contained an assembly and a NETCO-SNAP-IN insert). The initial case modeled the condition where all fuel assemblies are enclosed by inserts and was achieved by adding additional inserts§ along the top and left hand edges of the array in the outer water region. The comparison case modeled the more realistic condition where the additional inserts in the water region were removed. Based on this comparison the infinite lattice results will be increased by 0.001 Δk to account for this peripheral edge condition and to ensure conservative results are reported.

---

* 120 °C addresses the higher temperature conditions that are possible with fuel assemblies near the bottom of a 30 to 40 foot pool of water.

† This is because the storage array is over-moderated between the fuel assemblies.

‡ This analysis also supports the use of a standard 80 mil fuel channel.

§ The additional inserts were modeled outside of the storage rack array with the same overall spacing and orientation as the inserts in the storage rack cells.

The limiting conditions for the KENO rack calculations are shown in Table 6.2. Except as specifically noted, the reactivity values presented in Tables 6.1 and 6.2 do not include adjustments for uncertainties or code biases. Section 6.6 presents the determination of the upper limit 95/95 reactivity for the storage rack array.

6.4 *Uncertainties*

Uncertainties associated with defining bounding REBOL lattices are addressed in Appendix D. Specifically uncertainties associated with CASMO-4 code depletion and modeling capabilities are included within the REBOL definition process.

The unadjusted reactivity result reported in Table 6.2 is based upon the nominal bundle position and orientation in the storage rack shown in Figure 4.2. Simple rotation of the assembly or movement within the storage cell does not produce higher (statistically significant) results. As discussed in Section 6.3 a 0.001 Δk adder has been identified to account for the lack of B-10 absorber along 2 peripheral edges of the storage rack array. The manufacturing tolerance values and the calculated reactivity uncertainties for the ATRIUM-10 fuel are shown in Table 6.3. The gadolinia manufacturing uncertainty effect on reactivity was evaluated with a combination of KENO V.a and CASMO-4. All other uncertainties reported in Table 6.3 were evaluated with KENO V.a. The ATRIUM-10 rack calculations are conservatively performed for a minimum B10 areal density of the insert. BOL dimensions have been assumed, except the fuel rod pitch and channel bulge results are based upon conservative spacer and channel growth dimensions.*

6.5 *Abnormal and Accident Conditions*

In addition to the nominal storage cell arrangement, abnormal and accident conditions have also been considered. All Δk values provided in this section are based upon comparative KENO V.a calculations - only the most limiting scenario will be reflected in the $k_{95/95}$ calculation in Section 6.6.

For the misloaded assembly scenario, only the misplacement of a fuel assembly outside of and adjacent to the storage rack was analyzed because spent fuel pool rack drawings show that there is no gap between the racks wide enough to allow insertion of an assembly. No fuel

---

* The presence of activated corrosion and wear products (CRUD) is neglected because most of these compounds have higher neutron absorption cross sections than water.

channel was present on the misplaced assembly* and it was placed up against the stainless steel storage rack wall in a location where there is no neutron absorbing insert (see Figure 4.3) between the misplaced assembly and the adjacent assembly. Because this occurs on the edge of the rack array, where neutron leakage is high, only a small reactivity increase was observed (less than 0.001 Δk).

The situation where a single neutron absorbing insert is missing from an interior position of the storage rack was also evaluated. This was found to be the most reactive accident condition with a worth of 0.003 Δk.

The positioning of the assemblies within the storage cell was also evaluated for conditions with and without† a fuel channel. (This bounds the likely condition of an assembly being centered at the bottom and leaning against the storage cell wall at the top). Different configurations that pushed the assemblies toward each other in several combinations were investigated. The most reactive condition was found to occur when all assemblies are centered in the water region of the storage cell with a fuel channel installed. Since this is the nominal condition assumed for this analysis the effect of abnormal (or eccentric) assembly positioning is zero.

The orientation of the bundles within the storage rack is not restricted; therefore, the slightly asymmetric nature of the ATRIUM-10 fuel lattices has the potential to increase the pool reactivity if an optimal configuration is achieved. The 4 simple uniform rotation conditions were considered in Section 6.3, and 5 more complicated rotational combinations were evaluated as abnormal conditions. These complicated combinations investigated the effects of how rows, columns, and groups of assemblies could be oriented. From these cases, the worth of abnormal assembly orientation was found to be less than 0.001 Δk. This value is from a case where four rotation conditions are combined.

For the case of dropping a fuel assembly onto an assembly in the storage rack, the deformation of either assembly will not be sufficiently large to exceed the reactivity worth of these other limiting accident conditions. This is because it only involves 2 assemblies in a localized area. There will also be no effect on the array reactivity when the dropped assembly comes to rest in a horizontal or inclined position on top of the storage rack because the dropped assembly will

---

* To also evaluate minimum separation scenarios.

† To also evaluate minimum separation scenarios.

be neutronically isolated from the fuel in the storage cells (greater than 12 inches of water between the dropped assembly and the top of the active fuel zone of the fuel in the storage rack).

A dropped assembly falling into an empty storage cell would potentially deform the baseplate at the bottom of the storage cell. This could place the dropped assembly at a lower elevation than the other assemblies in the array which would decrease the array reactivity because of increased neutron leakage. If the impact deformed the dropped assembly a higher reactivity condition could be achieved; however, it would be bounded by these other limiting accident conditions because it is limited to a localized area.

6.6 *Determination of Maximum Rack Assembly k-eff*

For the ATRIUM-10 fuel design with REBOL lattice enrichments of 3.05 wt% U-235 (above 126"), 2.72 wt% U-235 (from 96" to 126"), and 2.66 wt% U-235 (from 0" to 96") , the maximum KENO calculated in-rack reactivity from Table 6.2 is 0.916. This k-eff value is used with the following equation to determine the upper limit 95/95 reactivity:

$$k_{95/95} = k_{eff} + bias_m + \Delta k_{sys} + (C^2\sigma_k^2 + C_m^2\sigma_m^2 + C^2\sigma_{sys}^2 + \Delta k_{tol}^2)^{1/2},$$

where:

k_{eff}	=	in-rack reactivity from KENO V.a, (0.916, Table 6.2)
$bias_m$	=	KENO V.a validation methodology bias (0.00542, page C-18)
Δk_{sys}	=	Summation of applicable system variables: maximum k-eff increase due to abnormal and accident conditions from Section 6.5 (0.003) and edge effect adder from Section 6.3 (0.001).
C	=	95% confidence level consistent with KENO V.a (2)
C_m	=	95/95 one-sided tolerance multiplier for a sample size of 100 (1.927)
σ_k	=	k-eff standard deviation from KENO V.a, (0.001, Table 6.2)
σ_m	=	KENO V.a methodology uncertainty (0.00511, page C-18)
σ_{sys}	=	$(\sigma_{sys1}^2 + \sigma_{sys2}^2 \ldots + \sigma_{sys\_n}^2)^{1/2}$, for Δk_{sys} uncertainties
Δk_{tol}	=	Statistical combination of manufacturing reactivity uncertainties (0.0105,Table 6.3)*

* The uncertainty value for non-ATRIUM-10 fuel types will not differ significantly.

The following table provides a summary of the Δk_{sys} and σ_{sys} parameters applicable to this analysis. (The σ values are standard deviation results from KENO)

Description	Δk_{sys}	σ_{sys}
Edge Effect (Insert Orientation, Section 6.3)	0.001	0.0007
Limiting Accident (Missing Insert, Section 6.5)	0.003	0.0006
Combined Values	0.004	0.0009

The standard deviations and tolerance uncertainties are included as the square root of the sum of the squares since they represent independent events. Solving for $k_{95/95}$ yields a 95/95 upper limit k-eff of 0.940. The above determination of the upper limit 95/95 k-eff is consistent with the method documented in Reference 8 and allows one to state that at least 95% of the normal population is less than the 95/95 k-eff value calculated with a 95% confidence.

The results demonstrate the postulated configuration with the ATRIUM-10 REBOL assembly lattices meets the NRC criticality safety acceptance criterion that the array k-eff under the worst credible conditions is ≤ 0.95. Since the REBOL infinite lattices have a higher reactivity than the reference bounding lattices as shown in Table 6.1, the reference bounding lattices also meet the k-eff ≤ 0.95 regulatory limit.

6.7 *Uniform vs. Distributed Enrichment Distributions*

A uniform enrichment distribution increases the BWR lattice reactivity because low enriched rods in the corners of the lattice are replaced with rods at an average enrichment level. Relative to the reference bounding lattices described in Table 6.1 a uniform enrichment distribution is more reactive by 0.005 to 0.007 Δk. This increase in reactivity is primarily due to increasing the enrichment in corner pins. This does not affect the results of this evaluation since a BWR assembly will always require low enrichments in the corners to maintain margin to LHGR and CPR limits.

6.8 *Arrays of Mixed BWR Fuel Types*

It is shown in Table B.1 that the ATRIUM-10 reference bounding lattices are equal to or more reactive in the in-rack configuration than the limiting lattices of the legacy fuel. Because the

GE14, ATRIUM-9, and ATRIUM-10 lattices have similar water and fuel characteristics the neutron energy spectra will be similar for these lattice types. Additionally, it is also shown in Table B.6 that the legacy 8x8 lattices have margin relative to the limiting lattices. It then follows that the ATRIUM-10 lattices used in this evaluation can reasonably represent past assembly fuel types.

The assembly enrichment and gadolinia limitations defined in Table 2.1 will be applied to all future ATRIUM-10 fuel assemblies that are built for LaSalle Unit 1 and Unit 2. Therefore, there will not be a more reactive assembly to consider in a misloaded assembly accident and an array composed of a mixture of these fuel types will not exceed the reactivity calculated for an array of limiting ATRIUM-10 assemblies.

6.9 *Inaccessible Storage Locations*

There are fuel storage locations around the edges of the LaSalle Unit 2 spent fuel pool which are physically inaccessible primarily due to crane interference with piping above the fuel storage racks. These locations will not contain an insert or a fuel assembly. The impact on the storage array k-eff was evaluated for different geometric configurations of empty storage locations without inserts.

The evaluation was performed using a 24X24 storage configuration. Originally all storage locations were fully loaded and contained inserts. Additional evaluations were completed with various storage locations containing neither fuel assemblies nor inserts. The locations and configurations evaluated are given in Table 6.4. These locations were selected to represent the irregular edge shape of the storage pool as well as configurations which could occur during the process of installing the inserts. For all cases the fully loaded array with inserts had the highest k-eff. The array reactivity is lower (by up to 0.002 Δk) with no neutron absorbing inserts and no fuel assemblies as defined by the geometries in Table 6.4. Therefore, empty cell locations without an assembly and without an insert do not increase the storage array k-eff.

6.10 *Interfaces between Areas with Different Storage Conditions*

As the inserts are installed the storage pool will become a mixture of degraded Boraflex regions and insert regions. The criticality safety evaluations for each of these loading configurations has demonstrated that on an independent (or single region) basis the storage pool multiplication factor is less than the 0.95 regulatory limit. The multiplication factor for a mixture of these

regions would be expected to also remain below 0.95 if the net transfer of neutrons from one region to another does not increase significantly.

Exelon commits to expand the placement of inserts into one row and one column of the adjacent region as necessary to completely surround all assemblies that are part of the insert region with four wings of the NETCO-SNAP-IN inserts*. As addressed in Section 6.8, the reactivity of future ATRIUM-10 fuel assemblies will not exceed the reference bounding assembly of this analysis. With these restrictions in place, the system k-eff of a pool comprised of insert regions mixed with degraded Boraflex regions will be lower than the maximum reported single region value. This occurs because replacement of a large portion of the storage area with another that has a lower multiplication factor decreases the multiplication factor of the entire storage area. KENO evaluations have demonstrated that the resulting k-eff for a system composed of two regions is between that of the individual systems composed of single regions.

The overall conclusion from this multi-region analysis is that the spent fuel pool will have a $k_{95/95}$ value less than or equal to 0.95. This conclusion is reached without crediting residual boron within the insert region.

* An exception to this would be peripheral regions of the rack that have no adjacent region.

Table 6.1 Summary of CASMO-4 Maximum Reactivity Results for the ATRIUM-10 Fuel Assembly

Characteristics of the Reference Bounding Fuel Lattices

ATRIUM-10 lattice
4.57 wt% U-235 distributed enrichment up to 126"
4.47 wt% U-235 distributed enrichment above 126"
10 gadolinia rods with 3.5 wt% Gd_2O_3 above 126" and 6.0 wt% Gd_2O_3 from 0" to 126"
Standard 100 mil Channel
No xenon in cold calculations
Top and bottom lattice geometry explicitly modeled
Reflective boundary for in-core
Periodic boundary for in-rack

Limiting Conditions

Top Lattice
Exposure 11.5 GWd/MTU
40% void history

Intermediate Lattice
Exposure 16.0 GWd/MTU
40% void history

Bottom Lattice
Exposure 16.5 GWd/MTU
40% void history

Calculated Bounding Lattice Reactivity

Condition	Maximum k_∞		
	Top Lattice	Intermediate Lattice	Bottom Lattice
In-Core, 20°C (68°F)	1.288	1.244	1.241
In-Rack*, 20°C (68°F)	0.917	0.886	0.883
In-Rack, 4°C (39.2°F)	0.9185	0.8869	0.8843

* In-Rack implies the Unit 2 spent fuel pool without Boraflex and with NETCO-SNAP-IN inserts.

Table 6.1 Summary of CASMO-4 Maximum Reactivity Results for the ATRIUM-10 Fuel Assembly *(Continued)*

REBOL Lattice Conditions

ATRIUM-10 top or bottom geometry with uniform enrichment distribution
3.05 wt% U-235 (above 126")
2.72 wt% U-235 (from 96" to 126")
2.66 wt% U-235 (from 0" to 96")
No gadolinia
BOL (zero exposure)
Standard 100 mil Channel
No xenon
Top and bottom lattice geometry explicitly modeled
Reflective boundary for in-core
Periodic boundary for in-rack

Calculated REBOL Lattice Reactivity

Condition	Maximum k_∞		
	Top Lattice	Intermediate Lattice	Bottom Lattice
In-Core, 20°C (68°F)	1.342	1.309	1.308
In-Rack*, 20°C (68°F)	0.926	0.895	0.892
In-Rack, 4°C (39.2°F)	0.929	0.898	0.895

* In-Rack implies the Unit 2 spent fuel pool without Boraflex and with NETCO-SNAP-IN inserts.

Table 6.2 Summary of KENO V.a Maximum In-Rack Reactivity for ATRIUM-10 Fuel

Fuel Assembly

ATRIUM-10 top geometry REBOL Lattice (above 126")
3.05 wt% U-235 uniform enrichment
ATRIUM-10 top geometry REBOL Lattice (96" to 126")
2.72 wt% U-235 uniform enrichment
ATRIUM-10 bottom geometry REBOL Lattice (from 0" to 96")
2.66 wt% U-235 uniform enrichment

No gadolinia
No xenon
Zero exposure
Standard 100 mil Channel*
Top and bottom lattice geometry explicitly modeled
Periodic boundary conditions

Storage Array Configuration

13x13 array with periodic boundary conditions in all directions
Storage cell pitch preserved across storage rack boundaries
Neutron absorbing, chevron shaped insert in each storage cell
Assembly centered in cell water volume (not centered relative to stainless steel box)
4°C moderator and fuel temperatures

Maximum Rack Reactivity

Description	k-eff
In-Rack 4°C (39.2°F) k-eff	0.916 ± 0.001
Maximum $k_{95/95}$ Reactivity (including uncertainties, biases, manufacturing tolerances and worst accident or abnormal loading conditions)	0.940

* Relative to array reactivity there is no significant difference between the 100 mil and the AREVA Advanced Fuel Channel.

Table 6.3 Manufacturing Reactivity Uncertainties

(Based upon BOL conditions using KENO V.a except as noted. Δk results of 0.0007 indicate cases where the differences were less than the uncertainty of the calculation)

Quantity	Nominal Value	Tolerance	Δk_∞
(Reactivity Uncertainty of Fuel Assembly Tolerance Values)			
Fuel rod pitch	0.510 in.	[ ]	
Fuel enrichment	4.57 wt% U235	[ ]	
Fuel density	96.26% TD	[ ]	
Channel bulge	0	[ ]	
Pellet diameter	0.3413 in.	[ ]	
Clad diameter - outer/inner	0.3957/0.3480 in.	[ ]	
Pellet void volume‡	1.2%	[ ]	--
Gadolinia concentration§	3.5 wt%	[ ]	
	6.0 wt%	[ ]	
(Reactivity Uncertainty of Rack Tolerance Values)			
Areal B-10 density	≥0.0086 g B10/cm^2	Min value was used	--
Insert thickness**	0.065 in.	±0.005 in.	--
SS wall thickness	0.090 in.	±0.009 in.	[ ]
Storage cell pitch	6.255 in.	[ ]	
Storage cell inside dimension	6.0 in.	±0.020 in.	[ ]
Statistical combination of uncertainties††			[ ]
Reported Value			0.0105

* Value is based upon component measurements at approximate peak reactivity exposures.

† This value is equally valid for a fuel density of 95.85% TD.

‡ This is an insignificant parameter; its effect was combined with the U235 enrichment result.

§ The gadolinia uncertainty Δk includes a CASMO-4 based 0.002 Δk adder which accounts for differences at peak reactivity conditions.

** Calculations confirmed that the storage vault reactivity is not affected by the thickness of the insert. This is expected because the B-10 density is defined as an areal density.

†† This is based upon the square root of the sum of the squares for all independent tolerance conditions.

Table 6.4 Evaluation for Inaccessible Storage Locations

Storage Cell Configuration* (X,Y)	Location within 24X24 array†
1x1	Center of array
2x2	Center of array
1X1	NE corner of array
4x1	NE corner of array
2x2	NE corner of array
1X4	NE corner of array
1X2	Center East side of array
2X1	Center East side of array
2x2	Center East side of array
3x3	Center East side of array
2x2	Center West side of array
1X4	SW corner of array
4X1	SW corner of array

* These locations do not contain a neutron absorbing insert or a fuel assembly.

† Locations (N, S ,E, or W) are relative to the computer model only.

7.0 Conclusions

This analysis demonstrates that all fuel assemblies delivered to the LaSalle Station (both Units 1 and 2) as of July 2009 can be safely stored in the LaSalle Unit 2 spent fuel pool with NETCO-SNAP-IN inserts. Future ATRIUM-10 fuel designs that meet the design requirements specified in Table 2.1 or that can be shown to be bounded by the reference bounding assembly can be safely stored in the LaSalle Unit 2 spent fuel pool. The array k-eff determined herein for the reference assembly, including all uncertainties, biases, manufacturing tolerances and worst accident or abnormal loading conditions is 0.940.

8.0 References

1. *Commonwealth Edison LaSalle Station Unit 2 Spent Fuel Storage Capacity Modification Safety Analysis Report*, 8601-00-0084, Revision 8, August 1986.

2. NUREG/CR-0200 Revision 6, *SCALE Version 4.4 A Modular Code System for Performing Standardized Computer Analyses for Licensing Evaluation,* Oak Ridge National Laboratory, May 2000.

3. NUREG/CR-6698, *Guide for Validation of Nuclear Criticality Safety Calculational Methodology,* Nuclear Regulatory Commission, January 2001.

4. US Tool and Die Drawing 8601-7 Revision 4, "Commonwealth Edison Co. LaSalle County Station Unit-2 Spent Fuel Storage Racks Fuel Box Assembly & Groups", released by Sargent & Lundy, April 1990.

5. NET-259-03 Revision 5, "Material Qualification of ALCAN Composite for Spent Fuel Storage," Northeast Technology Corp., July 2009.

6. Code of Federal Regulations, Title 10, Part 50, Section 68, "Criticality Accident Requirements."

7. NUREG-0800, *Standard Review Plan for the Review of Safety Analysis Reports for Nuclear Power Plants,* Section 9.1.1 Revision 3 (Criticality Safety of Fresh and Spent Fuel Storage and Handling), U.S. Nuclear Regulatory Commission, March 2007.

8. Design Requirements for Light Water Reactor Spent Fuel Storage Facilities at Nuclear Power Plants, ANSI/ANS American National Standard 57.2-1983, American Nuclear Society, October 1983, (withdrawn 1993).

9. Criticality Safety Criteria for the Handling, Storage and Transportation of LWR Fuel Outside Reactors, ANSI/ANS American National Standard 8.17-1984, American Nuclear Society, January 1984, (withdrawn 2004).

10. Letter, Brian K. Grimes, Assistant Director for Engineering and Projects Division of Operating Reactors, U.S. Nuclear Regulatory Commission, to All Power Reactor Licensees, "OT Position for the Review and Acceptance of Spent Fuel Storage and Handling Applications," April 14, 1978, as amended by letter, January 18, 1979.

11. Letter, Laurence Kopp (Reactor Systems Branch, NRC) to Timothy Collins, Chief (Reactor Systems Branch-NRC), Subject: "Guidance on the Regulatory Requirements for Criticality Analysis of Fuel Storage at Light-Water Reactor Power Plants," August 19, 1998.

12. EMF-2158(P)(A) Revision 0, *Siemens Power Corporation Methodology for Boiling Water Reactors: Evaluation and Validation of CASMO-4/MICROBURN-B2,* Siemens Power Corporation, October 1999.

Appendix A Sample CASMO-4 Input

Tables A.1, A.2, and A.3 provide the in-rack CASMO-4 models for the reference bounding lattices defined by this analysis.

ATRIUM-10 fuel which does not conform to the enrichment and gadolinia requirements described in Table 2.1 and Figure 2.1 can be analyzed for storage in the spent fuel pool racks by adapting the CASMO-4 sample inputs presented in Table A.1, A.2 or A.3. For bottom lattices the evaluation should be completed with both [ ] depletions. Intermediate and top lattices should be evaluated at both [ ] depletions. If the lifetime maximum in-rack k_∞ of the new lattice is less than the k_∞ of the corresponding reference bounding lattice, the ATRIUM-10 fuel assembly can be safely stored in the LaSalle Unit 2 Nuclear Power Station spent fuel storage rack.

If a different version of CASMO-4 is used, it is recommended that the sample cases for the reference bounding lattices (provided in Tables A.1 through A.3) be re-evaluated to establish that the version of CASMO-4 and the underlying libraries being used are consistent with those used in this report. Small changes, less than 0.005 Δk from the results in this report, are acceptable and can be used to establish new k_∞ limits for comparison to the new lattices (i.e. the comparison should be performed based upon the same calculational basis). Larger changes from the results contained in this report represent more significant changes in the underlying model and may require additional CASMO-4 to KENO benchmarking.

Table A.1 CASMO-4 Input for ATRIUM-10 Top Reference Bounding Lattice

```
TTL * A10T-4470L-10G35_BL - .40 VB
TFU= 814.3
TMO= 560.3
VOI=40
FUE, 1,10.42349/ 2.5000
FUE, 2,10.42349/ 3.4000
FUE, 3,10.42349/ 4.2000
FUE, 4,10.29433/ 4.4100,64016= 3.5000
FUE, 5,10.42349/ 4.6900
FUE, 6,10.42349/ 4.8000
FUE, 7,10.42349/ 4.9500
BWR,10,1.29540,13.40612,0.25400,0.66294,0.66294,1.2700,1
THE,0
FUM,0,2
PIN, 1,0.43345,0.44196,0.50254
PIN, 2,1.67767,1.75006/'MOD','BOX'//-9
PIN, 3,0.44196,0.50254/'COO','COO'
LPI
 1
 1 3
 1 1 1
 1 1 1 1
 1 3 1 1 2
 1 1 1 1 2 2
 1 1 1 1 2 2 2
 1 1 1 1 1 1 1 1
 1 3 1 1 1 3 1 1 3
 1 1 1 1 1 1 1 1 1 1
LFU
  1
  2  0
  3  7  7
  5  4  7  7
  5  0  7  7  0
  5  4  7  7  0  0
  5  7  7  7  0  0  0
  3  7  7  7  4  6  3  3
  2  0  7  4  7  0  4  7  0
  1  2  3  6  5  5  6  3  2  1
PDE,   51.9538, 'KWL'
DEP 0.0,0.1,0.5,1,1.5,2,2.5,3,3.5,4,4.5,5,5.5,6,6.5,7,7.5,8,8.5,9,9.5,10,10.5,
    11,11.5,12,12.5,13,13.5,14,14.5,15
STA
TTL *+LaSalle Rack at   4 deg. C (No BF with Boral Insert)
RES,,0,9,-15
VOI,00
TMO, 277.1 TFU, 277.1 PDE,0
CNU,'FUE',54135,1.0E-14
BCO 'PER'
GAP 4*0.49784
MI1 0.05209/5010=100.0
MI2 5.8408/347=94.89 1001=0.57 8000=4.54
FST  4*0.16510/4*0.32385/2*'MOD' 5*'MI1' 'MOD'/8*'MI2'/
STA
END
```

Table A.2 CASMO-4 Input for ATRIUM-10 Intermediate Reference Bounding Lattice

```
TTL * A10T-4570L-10G60_BL - .40 VB
TFU= 814.3
TMO= 560.3
VOI=40
FUE, 1,10.42349/ 2.5000
FUE, 2,10.42349/ 3.6000
FUE, 3,10.42349/ 4.4000
FUE, 4,10.20471/ 4.5500,64016= 6.0000
FUE, 5,10.42349/ 4.8000
FUE, 6,10.42349/ 4.9500
BWR,10,1.29540,13.40612,0.25400,0.66294,0.66294,1.2700,1
THE,0
FUM,0,2
PIN, 1,0.43345,0.44196,0.50254
PIN, 2,1.67767,1.75006/'MOD','BOX'//-9
PIN, 3,0.44196,0.50254/'COO','COO'
LPI
 1
 1 3
 1 1 1
 1 1 1 1
 1 3 1 1 2
 1 1 1 1 2 2
 1 1 1 1 2 2 2
 1 1 1 1 1 1 1 1
 1 3 1 1 1 3 1 1 3
 1 1 1 1 1 1 1 1 1 1
LFU
  1
  2  0
  3  6  6
  6  4  6  6
  6  0  6  6  0
  6  4  6  6  0  0
  6  6  6  6  0  0  0
  3  6  6  6  4  5  3  3
  2  0  6  4  6  0  4  6  0
  1  2  3  5  6  6  5  3  2  1
PDE,   51.9538, 'KWL'
DEP 0.0,0.1,0.5,1,1.5,2,2.5,3,3.5,4,4.5,5,5.5,6,6.5,7,7.5,8,8.5,9,9.5,10,10.5,
    11,11.5,12,12.5,13,13.5,14,14.5,15,15.5,16,16.5,17,17.5,18,18.5,19,19.5,20,
    20.5,21,21.5,22,22.5,23,23.5,24,24.5,25
STA
TTL *+LaSalle Rack at   4 deg. C (No BF with Boral Insert)
RES,,0,11,-25
VOI,00
TMO, 277.1 TFU, 277.1 PDE,0
CNU,'FUE',54135,1.0E-14
BCO 'PER'
GAP 4*0.49784
MI1 0.05209/5010=100.0
MI2 5.8408/347=94.89 1001=0.57 8000=4.54
FST  4*0.16510/4*0.32385/2*'MOD' 5*'MI1' 'MOD'/8*'MI2'/
STA
END
```

Table A.3 CASMO-4 Input for ATRIUM-10 Bottom Reference Bounding Lattice

```
TTL * A10B-4570L-10G60_BL - .40 VB
TFU= 791.6
TMO= 560.3
VOI=40
FUE, 1,10.42349/ 2.5000
FUE, 2,10.42349/ 3.6000
FUE, 3,10.42349/ 4.4000
FUE, 4,10.20471/ 4.4600,64016= 6.0000
FUE, 5,10.42349/ 4.8000
FUE, 6,10.42349/ 4.9500
BWR,10,1.29540,13.40612,0.25400,0.66294,0.66294,1.2700,1
THE,0
FUM,0,2
PIN, 1,0.43345,0.44196,0.50254
PIN, 2,1.67767,1.75006/'MOD','BOX'//-9
LPI
 1
 1 1
 1 1 1
 1 1 1 1
 1 1 1 1 2
 1 1 1 1 2 2
 1 1 1 1 2 2 2
 1 1 1 1 1 1 1 1
 1 1 1 1 1 1 1 1 1
 1 1 1 1 1 1 1 1 1 1
LFU
  1
  2  3
  3  6  6
  6  4  6  6
  6  6  6  6  0
  6  4  6  6  0  0
  6  6  6  6  0  0  0
  3  6  6  6  4  5  3  3
  2  3  6  4  6  6  4  6  3
  1  2  3  5  6  6  5  3  2  1
PDE,   51.9538, 'KWL'
DEP 0.0,0.1,0.5,1,1.5,2,2.5,3,3.5,4,4.5,5,5.5,6,6.5,7,7.5,8,8.5,9,9.5,10,10.5,
    11,11.5,12,12.5,13,13.5,14,14.5,15,15.5,16,16.5,17,17.5,18,18.5,19,19.5,20,
    20.5,21,21.5,22,22.5,23,23.5,24,24.5,25
STA
TTL *+LaSalle Rack at   4 deg. C (No BF with Boral Insert)
RES,,0,11,-25
VOI,00
TMO, 277.1 TFU, 277.1 PDE,0
CNU,'FUE',54135,1.0E-14
BCO 'PER'
GAP 4*0.49784
MI1 0.05209/5010=100.0
MI2 5.8408/347=94.89 1001=0.57 8000=4.54
FST  4*0.16510/4*0.32385/2*'MOD' 5*'MI1' 'MOD'/8*'MI2'/
STA
END
```

Appendix B Reactivity Comparison for Assemblies Used in the LaSalle Reactors

The following tables present a comparison of in-rack CASMO-4 k_∞ values* (without Boraflex and with NETCO-SNAP-IN inserts) of the more reactive lattices of the different fuel assembly types used at or manufactured for the LaSalle Unit 1 or Unit 2 reactors prior to July 2009. For each assembly type, the more reactive lattices have been identified using a comparison of the U235 enrichment levels and the gadolinia concentrations. The comparisons are made based on three axial zones, 0" to 96", 96" to 126", and 126" to 149". The ATRIUM-9 458L-8G6 lattice is the most reactive as-fabricated design from 0" to 96" and from 96" to 126", and the ATRIUM-10T-4444L-12G40 lattice is the most reactive as fabricated design from 126" to 149". In the following tables LSA and LSB refer to LaSalle unit 1 or 2, respectively.

The following comparison table shows that the ATRIUM-10 reference bounding lattices described in Table 6.1 are equal to or more reactive than any of the lattices used in the LaSalle reactors. (Also note that the REBOL lattices used in the KENO V.a calculations are more reactive than the reference bounding lattices).

* [

]

Table B.1 Lattice Reactivity Comparisons (REBOL, Bounding, and Limiting)

Case Description	Lattice Description	Maximum In-Rack k_∞ (CASMO-4)	
		4 °C	20 °C
REBOL, Top Lattice 126" to 149"	A10T-305L0G0	0.929	0.926
Reference Bounding Top Lattice 126" to 149"	A10T-447L10G35	0.919	0.917
Limiting As-Fabricated Top Lattice 126" to 149"	A10T-4444L12G40	0.907	0.906
REBOL, Intermediate Lattice 96" to 126"	A10T-272L0G0	0.898	0.895
Reference Bounding Intermediate Lattice 96" to 126"	A10T-457L10G60	0.887	0.886
Limiting As-Fabricated Intermediate Lattice 96" to 126"	A9-458L8G6	0.884	0.883
REBOL, Bottom Lattice 0" to 96"	A10B-266L0G0	0.895	0.892
Reference Bounding Bottom Lattice 0" to 96"	A10B-457L10G60	0.884	0.883
Limiting As-Fabricated Bottom Lattice 0" to 96"	A9-458L8G6	0.884	0.883

Table B.2 ATRIUM-10 Fuel Lattice Reactivity Comparison

Case*	Lattice†	Maximum In-Rack k_∞ (CASMO-4)			Unit and Cycle Loaded
		4 °C	20 °C	100 °C	
T	A10T-4444L12G40	0.907	0.906	0.895	---
1	A10T-2111L0G0	0.825	0.822	0.803	LSB Cy10
2	A10T-3947L13G38	0.882	0.881	0.870	LSB Cy13
3	A10T-4444L12G40	0.907	0.906	0.895	LSA Cy13
4	A10T-4409L10G45	0.907	0.905	0.895	LSB Cy12
4a	A10T-4400L10G45	0.907	0.905	0.895	LSA Cy12
I	A9-458L8G6	0.884	0.883	0.875	---
1	A10T-2111L0G0	0.825	0.822	0.803	LSB Cy10
5	A10T-4313L15G65	0.860	0.859	0.850	LSB Cy10
6	A10T-4524L13GV70	0.860	0.858	0.849	LSB Cy13
7	A10T-4511L15GV80	0.840	0.839	0.830	LSB Cy13

* T, I, and B indicate the most reactive top, intermediate, and bottom lattice cases, respectively.

† Note that A10T and A10B indicate top and bottom ATRIUM-10 lattice geometry. A9 indicates ATRIUM-9.

Table B.2 ATRIUM-10 Fuel Lattice Reactivity Comparison *(Continued)*

Case*	Lattice†	Maximum In-Rack k_∞ (CASMO-4)			Unit and Cycle Loaded
		4 °C	20 °C	100 °C	
B	A9-458L8G6	0.884	0.883	0.875	---
8	A10B-1831L-0G0	0.785	0.782	0.764	LSB Cy10
9	A10B-4399L12G65	0.871	0.869	0.860	LSA Cy13
10	A10B-4537L13GV70	0.857	0.856	0.847	LSB Cy13
11	A10B-4510L13G75	0.863	0.862	0.853	LSA Cy10
12	A10B-4538L13GV80	0.844	0.843	0.834	LSB Cy13

* T, I, and B indicate the most reactive top, intermediate, and bottom lattice cases, respectively.

† Note that A10T and A10B indicate top and bottom ATRIUM-10 lattice geometry. A9 indicates ATRIUM-9.

Table B.3 ATRIUM 10XM Fuel Lattice Reactivity Comparison

Case*	Lattice†	Maximum In-Rack k_∞ (CASMO-4)			Unit and Cycle Loaded
		4 °C	20 °C	100 °C	
T	A10T-4444L12G40	0.907	0.906	0.895	---
1	DXMT-4056L12G40	0.880	0.879	0.869	LSB Cy13‡
I	A9-458L8G6	0.884	0.883	0.875	---
2	DXMT-4176L14GV60	0.852	0.851	0.842	LSB Cy13
B	A9-458L8G6	0.884	0.883	0.875	---
2	DXMT-4176L14GV60	0.852	0.851	0.842	LSB Cy13
3	DXMB-4365L14GV80	0.840	0.839	0.830	LSB Cy13

* T, I, and B indicate the most reactive top, intermediate, and bottom lattice cases, respectively.

† Note that A10T and A10B indicate top and bottom ATRIUM-10 lattice geometry. A9 indicates ATRIUM-9.

‡ 8 ATRIUM 10XM lead use assemblies have been manufactured as part of the reload fuel for LaSalle Unit 2 Cycle 13.

Table B.4 ATRIUM-9 Fuel Lattice Reactivity Comparison

Case*	Lattice†	Maximum In-Rack k_∞ (CASMO-4)			Unit and Cycle Loaded
		4 °C	20 °C	100 °C	
T	A10T-4444L12G40	0.907	0.906	0.895	---
I & B	A9-458L8G6	0.884	0.883	0.875	---
1	A9-396L8G5	0.875	0.874	0.865	LSA&B Cy9
2	A9-458L8G6	0.884	0.883	0.875	LSA&B Cy9
3	A9-459L12G7	0.870	0.869	0.861	LSA Cy9
4	A9-459L12G8	0.858	0.857	0.850	LSA Cy9

* T, I, and B indicate the most reactive top, intermediate, and bottom lattice cases, respectively.

† Note that A10T indicates top ATRIUM-10 lattice geometry and A9 indicates ATRIUM-9.

Table B.5 GE14 Fuel Lattice Reactivity Comparison

Case*	Lattice†	Maximum In-Rack k_∞ (CASMO-4)			Unit and Cycle Loaded
		4 °C	20 °C	100 °C	
T	A10T-4444L12G40	0.907	0.906	0.895	---
1	GE14-429L6G70-9G60	0.849	0.847	0.838	LSB Cy11
2	GE14-430L2G80-7G70-5G60	0.844	0.843	0.834	LSB Cy11
3	GE14-446L-10G80-4G70	0.844	0.842	0.834	LSA Cy11
I	A9-458L8G6	0.884	0.883	0.875	---
1	GE14-429L6G70-9G60	0.849	0.847	0.838	LSB Cy11
2	GE14-430L2G80-7G70-5G60	0.844	0.843	0.834	LSB Cy11
3	GE14-446L-10G80-4G70	0.844	0.842	0.834	LSA Cy11
B	A9-458L8G6	0.884	0.883	0.875	---
4	GE14-435L6G70-9G60	0.841	0.840	0.830	LSB Cy11
5	GE14-437L2G80-7G70-5G60	0.834	0.832	0.823	LSB Cy11
6	GE14-451L10G80-4G70	0.834	0.833	0.824	LSA Cy11
6a	GE14-451L11G80-4G70	0.842	0.841	0.832	LSA Cy11

* T, I, and B indicate the most reactive top, intermediate, and bottom lattice cases, respectively.

† Note that A10T indicates top ATRIUM-10 lattice geometry and A9 indicates ATRIUM-9. GE14 indicates GE14 geometry.

Table B.6 GE 8x8 Fuel Lattice Reactivity Comparison

Case*	Lattice†	Maximum In-Rack k_∞ (CASMO-4)			Unit and Cycle Loaded
		4 °C	20 °C	100 °C	
T	A10T-4444L12G40	0.907	0.906	0.895	---
I & B	A9-458L8G6	0.884	0.883	0.875	---
1	8x8_2-319L6G30	0.858	0.857	0.844	LSB Cy3
2	8x8_2-340L7G30	0.869	0.867	0.855	LSB Cy3
3	8x8_4-338L7G30	0.863	0.861	0.850	LSB Cy5
4	8x8_4-388L8G40	0.875	0.874	0.863	LSA Cy8

* T, I, and B indicate the most reactive top, intermediate, and bottom lattice cases, respectively.

† Note that A10T indicates top ATRIUM-10 lattice geometry and A9 indicates ATRIUM-9. 8x8_2 implies an 8x8 lattice with 2 water rods and 8x8_4 indicates an 8x8 lattice with a large internal water rod encompassing the area of 4 pin cells, i.e. GE9 fuel.

Appendix C KENO V.a Bias and Bias Uncertainty Evaluation

The purpose of the present analysis is to determine the bias of the k_{eff} calculated with the SCALE 4.4a computer code for spent fuel pool criticality analysis. A statistical methodology is used to evaluate criticality benchmark experiments that are appropriate for the expected range of parameters. The scope of this report is limited to the validation of the KENO V.a module and CSAS25 driver in the SCALE 4.4a code package for use with the 44 energy group cross-section library 44GROUPNDF5 for spent fuel criticality analyses.

This calculation is performed according to the general methodology described in Reference C.2 (NUREG/CR-6698 "Guide for Validation of Nuclear Criticality Safety Calculational Methodology") that is also briefly described in Section C.1. The critical experiments selected to benchmark the computer code system are discussed in Section C.3. The results of the criticality benchmark calculations, the trending analysis, the basis for the statistical technique chosen, the bias, and the bias uncertainty are presented in Sections C.4—C.7. Final results are summarized in Section C.8.

C.1 Statistical Method for Determining the Code Bias

As presented in Reference C.2 (NUREG/CR-6698), the validation of the criticality code must use a statistical analysis to determine the bias and bias uncertainty in the calculation of k_{eff}. The approach involves determining a weighted mean of k_{eff} that incorporates the uncertainty from both the measurement (σ_{exp}) and the calculation method (σ_{calc}). A combined uncertainty can be determined using the Equation 3 from Reference C.2, for each critical experiment:

$$\sigma_t = (\sigma_{calc}^2 + \sigma_{exp}^2)^{1/2}$$

The weighted mean of k_{eff} ($\bar{k}_{eff}$), the variance about mean (s), and the average total uncertainty of the benchmark experiments ($\bar{\sigma}^2$) can be calculated using the weighting factor $1/\sigma_t^2$ (see Eq. 4, 5, and 6 in Reference C.2). The final objective is to determine the square root of the pooled variance, defined as (Eq. 7 from Reference C.2):

$$s_P = \sqrt{s^2 + \bar{\sigma}^2}$$

The above value is used as the mean bias uncertainty, where bias is determined by the relation:

$Bias = \bar{k}_{eff} - 1$, if $\bar{k}_{eff}$ is less than 1, otherwise Bias = 0 (Eq.8 from Reference C.2)

The approach for determining the final statistical uncertainty in the calculational bias relies on the selection of an appropriate statistical treatment. Basically, the same steps and methods suggested in Reference C.2 for determining the upper safety limit (USL) can be applied also for determining the final bias uncertainty.

First, the possible trends in bias need to be investigated. Trends are identified through the use of regression fits to the calculated k_{eff} results. In many instances, a linear fit is sufficient to determine a trend in bias. Typical parameters used in these trending analyses are enrichment, H/X or a generic spectral parameter such as the energy of the average lethargy causing fission (EALF).

Reference C.2 indicates that the use of both weighted or unweighted least squares techniques is an appropriate means for determining the fit of a function. For the present analysis linear regression was used on both weighted and unweighted k_{eff} values to determine the existence of a trend in bias. Typical numerical goodness of fit tests were applied afterwards to confirm the validity of the trend.

When a relationship between a calculated k_{eff} and an independent variable can be determined, a one-sided lower tolerance band may be used to express the bias and its uncertainty (Reference C.2). When no trend is identified, the pool of k_{eff} data is tested for normality. If the data is normally distributed, then a technique such as a one-sided tolerance limit is used to determine bias and its uncertainty. If the data is not normally distributed, then a non-parametric analysis method must be used to determine the bias and its uncertainty (Reference C.2). Similar examples of application of these techniques are included in References C.4 and C.5.

C.2 Area of Applicability Required for the Benchmark Experiments

BWR spent fuel pools will primarily contain commercial nuclear fuel in uranium oxide pins in a square array. This fuel is characterized by the typical parameter values provided in Table C.1. These typical values were used as primary tools in selecting the benchmark experiments appropriate for determining the code bias.

Benchmark calculations have been made on selected critical experiments, chosen, in so far as possible, to bound the range of variables in the spent fuel rack analyses. In rack designs, the most significant parameters affecting criticality are: (1) the fuel enrichment, (2) the ^{10}B loading in the neutron absorber, and (3) the lattice spacing. Other parameters have a smaller effect but have been also included in the analyses.

One possible way of representing the data is through a spectral parameter that incorporates influences from the variations in other parameters. Such a parameter is computed by KENO V.a, which prints the "energy of the average lethargy causing fission" (EALF). The expected range for this parameter in the analyses was also included in Table C.1.

Table C.1 Range of Values of Key Parameters in Spent Fuel Pool

Parameter	Range of Values
Fissile material – Physical/Chemical Form	UO_2 rods
Enrichment	natural to 5.00 wt% U-235
Moderation/Moderator	Heterogeneous/Water
Lattice	Square
Pitch	1.2 to 1.45 cm
Clad	Zircaloy
Anticipated Absorber/Materials	Aluminum, Boron Stainless Steel
H/X ratio	0 to 473
Reflection	Water, Stainless Steel
Neutron Energy Spectrum (Energy of the Average Lethargy Causing Fission)	0.1 to 2.5 eV

C.3 Description of the Criticality Experiments Selected

The set of criticality benchmark experiments has been constructed to accommodate large variations in the range of parameters of the rack configurations and also to provide adequate statistics for the evaluation of the code bias.

One hundred critical configurations were selected from various sources. These benchmarks include configurations performed with lattices of UO_2 fuel rods in water having various enrichments and moderating ratios (H/X). A set of MOX criticality benchmarks is also included in the present set. The area of applicability (AOA) is established within this range of benchmark experiment parameter values.

A brief description of the selected benchmark experiments is presented in Table C.2. The table includes the references where detailed descriptions of the experiments are presented.

Table C.2 Descriptions of the Critical Benchmark Experiments

Experiment Case Name	Measure d k_{eff}	σ exp	Brief Description	Neutron Absorber	Reflector
NUREG/CR-0073 PNL experiments (Reference C.3)					
c004	1.0000	0.0020	UO_2 pellets with 4.31 wt% ^{235}U Cluster of fuel rods on a 25.4 mm pitch. Moderator; water or borated water. Various separation distances used between clusters. Those so indicated have plates of neutron absorbing material poison placed between clusters of fuel rods.	None	Water and acrylic plates as well as a biological shield serve as primary reflector material. A minor contribution comes from the channel that supports the rod clusters and the 9.52 mm carbon steel tank wall.
c005b	1.0000	0.0018		0.625 cm Al plates	
c006b	1.0000	0.0019		0.625 cm Al plates	
c007a	1.0000	0.0021		0.302 cm SS-304L plates	
c008b	1.0000	0.0021		0.298 cm SS-304L absorber plates with 1.05 wt % or 1.62 wt% B	
c009b	1.0000	0.0021			
c010b	1.0000	0.0021			
c011b	1.0000	0.0021			
c012b	1.0000	0.0021			
c013b	1.0000	0.0021		0.485 cm SS304L plates	
c014b	1.0000	0.0021			
c029b	1.0000	0.0021		Zircaloy-4 absorber plates	
c030b	1.0000	0.0021			
c031b	1.0000	0.0021		Boral absorber	
BAW-1484-7 experiments (Reference C.4)					
aclp1	1.0002	0.0005	Enrichments of 2.459 wt% ^{235}U 3x3 array of fuel clusters. Various B_4C pins and stainless steel and boron-aluminum sheets were used as neutron absorbers. Cases so indicated also had dissolved boron in the water moderator.	None	Water and aluminum base plate are the primary reflective materials in the experiments. Minor contribution from the steel tank walls.
aclp2	1.0001	0.0005		1037 ppm boron	
aclp3	1.0000	0.0006		764 ppm boron	
aclp4	0.9999	0.0006		None	
aclp5	1.0000	0.0007		None	
aclp6	1.0097	0.0012		None	
aclp7	0.9998	0.0009		None	
aclp8	1.0083	0.0012		None	
aclp9	1.0030	0.0009		None	
aclp10	1.0001	0.0009		143 ppm boron	
aclp11a	1.0000	0.0006		510 ppm boron	
aclp11b	1.0007	0.0007		514 ppm boron	
aclp11c	1.0007	0.0006		501 ppm boron	
aclp11d	1.0007	0.0006		493 ppm boron	
aclp11e	1.0007	0.0006		474 ppm boron	
aclp11f	1.0007	0.0006		462 ppm boron	
aclp11g	1.0007	0.0006		432 ppm boron	
aclp12	1.0000	0.0007		217 ppm boron	
aclp13	1.0000	0.0010		15 ppm boron	
aclp13a	1.0000	0.0010		28 ppm boron	
aclp14	1.0001	0.0010		92 ppm boron	
aclp15	0.9998	0.0016		395 ppm boron	
aclp16	1.0001	0.0019		121 ppm boron	
aclp17	1.0000	0.0010		487 ppm boron	
aclp18	1.0002	0.0011		197 ppm boron	
aclp19	1.0002	0.0010		634 ppm boron	
aclp20	1.0003	0.0011		320 ppm boron	
aclp21	0.9997	0.0015		72 ppm boron	

BAW-1645-4 experiments (Reference C.5)					
rcon01	1.0007	0.0006	2.46 wt% ^{235}U 5x5 array of fuel cluster. Rod pitch between 1.2093 cm and 1.4097 cm. Cases so indicated also had dissolved boron in the water moderator.	435 ppm boron	Water and aluminum base plate are the primary reflective materials in the experiments. Minor contribution from the steel tank walls.
rcon02	1.0007	0.0006		426 ppm boron	
rcon03	1.0007	0.0006		406 ppm boron	
rcon04	1.0007	0.0006		383 ppm boron	
rcon05	1.0007	0.0006		354 ppm boron	
rcon06	1.0007	0.0006		335 ppm boron	
rcon07	1.0007	0.0006		361 ppm boron	
rcon08	1.0007	0.0006		121 ppm boron	
rcon09	1.0007	0.0006		886 ppm boron	
rcon10	1.0007	0.0006		871 ppm boron	
rcon11	1.0007	0.0006		852 ppm boron	
rcon12	1.0007	0.0006		834 ppm boron	
rcon13	1.0007	0.0006		815 ppm boron	
rcon14	1.0007	0.0006		781 ppm boron	
rcon15	1.0007	0.0006		746 ppm boton	
rcon16	1.0007	0.0006		1156 ppm boron	
rcon17	1.0007	0.0006		1141 ppm boron	
rcon18	1.0007	0.0006		1123 ppm boron	
rcon19	1.0007	0.0006		1107 ppm boron	
rcon20	1.0007	0.0006		1093 ppm boron	
rcon21	1.0007	0.0006		1068 ppm boron	
rcon28	1.0007	0.0006		121 ppm boron	
CEA Valduc Critical Mass Laboratory Experiments (Reference C.6)					
mdis01	1.0000	0.0014	4.738 wt% ^{235}U CEA Valduc Critical Mass Laboratory experiments. A key aspect of these experiments was to examine the reactivity effects of differing densities of hydrogenous materials within a cross shaped channel box placed between a two by two array of fuel rod assemblies. The assemblies each consisted of an 18 x 18 array of aluminum alloy clad fuel UO2 pellet columns.	None	The actual reflector boundaries vary from case to case.
mdis02	1.0000	0.0014			
mdis03	1.0000	0.0014			
mdis04	1.0000	0.0014			
mdis05	1.0000	0.0014			
mdis06	1.0000	0.0014			
mdis07	1.0000	0.0014			
mdis08	1.0000	0.0014			
mdis09	1.0000	0.0014			
mdis10	1.0000	0.0014			
mdis11	1.0000	0.0014			
mdis12	1.0000	0.0014			
mdis13	1.0000	0.0014			
mdis14	1.0000	0.0014			
mdis15	1.0000	0.0014			
mdis16	1.0000	0.0014			
mdis17	1.0000	0.0014			
mdis18	1.0000	0.0014			
mdis19	1.0000	0.0014			

LEU-COMP-THERM-022, -024, -025 Experiments (Reference C.1)					
leuct022-02	1.0000	0.0046	9.83 and 7.41 wt% enriched UO2 rods of varying numbers in hexagonal and square lattices in water.	None	Water is the primary reflector. Minor contribution from the steel tank walls.
leuct022-03	1.0000	0.0036			
leuct024-01	1.0000	0.0054			
leuct024-02	1.0000	0.0040			
leuct025-01	1.0000	0.0041			
leuct025-02	1.0000	0.0044			
Mixed Oxide (Reference C.1, Experiment MIX-COMP-THERM 002)					
epri70b (PNL-31)	1.0009	0.0047	Experiments with mixtures of natural UO2-2wt%PuO2 (8%240Pu). Square pitched lattices, with 1.778 cm, 2.2098 cm, and 2.5146 cm pitch in borated or pure water moderator.	687.9 ppm B	Reflected by water and Al.
epri70un (PNL-30)	1.0024	0.0060		1.7 ppm B	
epri87b (PNL-33)	1.0024	0.0024		1090.4 ppm B	
epri87un (PNL-32)	1.0042	0.0031		0.9 ppm B	
epri99b (PNL-35)	1.0029	0.0027		767.2 ppm B	
epri99un (PNL-34)	1.0038	0.0025		1.6 ppm B	
Mixed Oxide (Reference C.1, Experiment MIX-COMP-THERM 003)					
saxtn104 (case 6)	1.0000	0.0023	Experiments with mixtures of natural UO2-6.6wt%PuO2 mixed-oxide (MOX), square-pitched, partial moderator height lattices. Moderator: borated or pure water moderator.	None	Reflected by water and Al.
saxtn56b (case 3)	1.0000	0.0054		337 ppm B	
saxtn792 (case 5)	1.0049	0.0027		None	
saxton52 (case 1)	1.0028	0.0072		None	
saxton56 (case 2) (PNL-35)	1.0019	0.0059		None	

C.4 Results of Calculations with SCALE 4.4.a

The critical experiments described in Section C.3 were modeled with the SCALE 4.4a computer system. The resulting k_{eff} and calculational uncertainty, along with the experimental k_{eff} and experimental uncertainty are tabulated in Table C.3. The parameters of interest in performing a trending analysis of the bias (Including EALF calculated by SCALE 4.4a) are also included in the table.

Table C.3 SCALE 4.4a Results for the Selected Benchmark Experiments

No	Case name	Benchmark values		SCALE 4.4a Calculated Values		EALF (eV)	Enr wt% ^{235}U	B (ppm)	H/X
		k_{eff}	σ_{exp}	k_{eff}	σ_{calc}				
1	c004	1.0000	0.0020	0.9966	0.0008	0.1126	4.31	0	255.92
2	c005b	1.0000	0.0018	0.9950	0.0008	0.1128	4.31	0	255.92
3	c006b	1.0000	0.0019	0.9964	0.0008	0.1130	4.31	0	255.92
4	c007a	1.0000	0.0021	0.9973	0.0009	0.1128	4.31	0	255.92
5	c008b	1.0000	0.0021	0.9966	0.0008	0.1135	4.31	0	255.92
6	c009b	1.0000	0.0021	0.9967	0.0008	0.1136	4.31	0	255.92
7	c010b	1.0000	0.0021	0.9977	0.0008	0.1142	4.31	0	255.92
8	c011b	1.0000	0.0021	0.9949	0.0009	0.1143	4.31	0	255.92
9	c012b	1.0000	0.0021	0.9967	0.0008	0.1148	4.31	0	255.92
10	c013b	1.0000	0.0021	0.9969	0.0008	0.1130	4.31	0	255.92
11	c014b	1.0000	0.0021	0.9958	0.0008	0.1133	4.31	0	255.92
12	c029b	1.0000	0.0021	0.9972	0.0008	0.1126	4.31	0	255.92
13	c030b	1.0000	0.0021	0.9972	0.0009	0.1132	4.31	0	255.92
14	c031b	1.0000	0.0021	0.9993	0.0009	0.1144	4.31	0	255.92
15	aclp1	1.0002	0.0005	0.9912	0.0007	0.1725	2.46	0	215.57
16	aclp2	1.0001	0.0005	0.9951	0.0006	0.2504	2.46	1037	215.79
17	aclp3	1.0000	0.0006	0.9958	0.0006	0.1963	2.46	764	215.83
18	aclp4	0.9999	0.0006	0.9889	0.0008	0.1912	2.46	0	215.91
19	aclp5	1.0000	0.0007	0.9906	0.0007	0.1660	2.46	0	215.87
20	aclp6	1.0097	0.0012	0.9899	0.0009	0.1712	2.46	0	215.87
21	aclp7	0.9998	0.0009	0.9891	0.0008	0.1496	2.46	0	215.87
22	aclp8	1.0083	0.0012	0.9873	0.0007	0.1537	2.46	0	215.87
23	aclp9	1.0030	0.0009	0.9908	0.0008	0.1409	2.46	0	215.87
24	aclp10	1.0001	0.0009	0.9916	0.0007	0.1495	2.46	143	215.22
25	acp11a	1.0000	0.0006	0.9948	0.0007	0.1996	2.46	510	215.32
26	acp11b	1.0007	0.0007	0.9947	0.0007	0.1994	2.46	514	215.73
27	acp11c	1.0007	0.0006	0.9944	0.0006	0.2019	2.46	501	215.32
28	acp11d	1.0007	0.0006	0.9952	0.0007	0.2028	2.46	493	215.14
29	acp11e	1.0007	0.0006	0.9940	0.0006	0.2037	2.46	474	214.70
30	acp11f	1.0007	0.0006	0.9932	0.0007	0.2050	2.46	462	214.52
31	acp11g	1.0007	0.0006	0.9954	0.0007	0.2045	2.46	432	215.97
32	aclp12	1.0000	0.0007	0.9930	0.0008	0.1700	2.46	217	215.05
33	aclp13	1.0000	0.0010	0.9933	0.0008	0.1965	2.46	15	215.67
34	acp13a	1.0000	0.0010	0.9902	0.0007	0.1981	2.46	28	215.91
35	aclp14	1.0001	0.0010	0.9891	0.0008	0.2011	2.46	92	215.83
36	aclp15	0.9998	0.0016	0.9855	0.0007	0.2063	2.46	395	215.83
37	aclp16	1.0001	0.0019	0.9856	0.0007	0.1730	2.46	121	215.83
38	aclp17	1.0000	0.0010	0.9899	0.0006	0.2053	2.46	487	215.89
39	aclp18	1.0002	0.0011	0.9886	0.0008	0.1725	2.46	197	215.89
40	aclp19	1.0002	0.0010	0.9912	0.0006	0.2061	2.46	634	215.89
41	aclp20	1.0003	0.0011	0.9899	0.0007	0.1730	2.46	320	215.89
42	aclp21	0.9997	0.0015	0.9883	0.0008	0.1532	2.46	72	216.19
43	rcon01	1.0007	0.0006	0.9997	0.0007	2.4282	2.46	435	17.41
44	rcon02	1.0007	0.0006	1.0004	0.0007	2.4360	2.46	426	17.40
45	rcon03	1.0007	0.0006	0.9985	0.0008	2.4972	2.46	406	17.40
46	rcon04	1.0007	0.0006	0.9983	0.0007	2.4989	2.46	383	17.41
47	rcon05	1.0007	0.0006	1.0002	0.0007	2.4988	2.46	354	17.41

No	Case name	Benchmark values		SCALE 4.4a Calculated Values		EALF (eV)	Enr wt% ^{235}U	B (ppm)	H/X
		k_{eff}	σ_{exp}	k_{eff}	σ_{calc}				
48	rcon06	1.0007	0.0006	0.9982	0.0007	2.5119	2.46	335	17.41
49	rcon07	1.0007	0.0006	0.9984	0.0006	1.6313	2.46	361	17.43
50	rcon08	1.0007	0.0006	1.0155	0.0008	1.1134	2.46	121	17.43
51	rcon09	1.0007	0.0006	0.9973	0.0007	1.4481	2.46	886	44.81
52	rcon10	1.0007	0.0006	0.9982	0.0008	1.4623	2.46	871	44.81
53	rcon11	1.0007	0.0006	0.9958	0.0007	1.5006	2.46	852	44.79
54	rcon12	1.0007	0.0006	0.9979	0.0007	1.4942	2.46	834	44.81
55	rcon13	1.0007	0.0006	0.9971	0.0006	1.4973	2.46	815	44.81
56	rcon14	1.0007	0.0006	0.9967	0.0007	1.5185	2.46	781	44.79
57	rcon15	1.0007	0.0006	0.9980	0.0006	1.5122	2.46	746	44.79
58	rcon16	1.0007	0.0006	0.9954	0.0006	0.4182	2.46	1156	118.47
59	rcon17	1.0007	0.0006	0.9963	0.0007	0.4293	2.46	1141	118.47
60	rcon18	1.0007	0.0006	0.9929	0.0007	0.4354	2.46	1123	118.44
61	rcon19	1.0007	0.0006	0.9952	0.0007	0.4371	2.46	1107	118.44
62	rcon20	1.0007	0.0006	0.9952	0.0007	0.4367	2.46	1093	118.44
63	rcon21	1.0007	0.0006	0.9945	0.0007	0.4404	2.46	1068	118.44
64	rcon28	1.0007	0.0006	0.9970	0.0008	0.9984	2.46	121	17.44
65	mdis01	1.0000	0.0014	0.9929	0.0008	0.2822	4.74	0	137.61
66	mdis02	1.0000	0.0014	0.9862	0.0009	0.2641	4.74	0	137.61
67	mdis03	1.0000	0.0014	0.9845	0.0009	0.2636	4.74	0	137.61
68	mdis04	1.0000	0.0014	0.9895	0.0008	0.2513	4.74	0	137.61
69	mdis05	1.0000	0.0014	0.9901	0.0009	0.2411	4.74	0	137.61
70	mdis06	1.0000	0.0014	1.0010	0.0008	0.2292	4.74	0	137.61
71	mdis07	1.0000	0.0014	0.9901	0.0009	0.2250	4.74	0	137.61
72	mdis08	1.0000	0.0014	0.9858	0.0008	0.2493	4.74	0	137.61
73	mdis09	1.0000	0.0014	0.9856	0.0009	0.2483	4.74	0	137.61
74	mdis10	1.0000	0.0014	0.9928	0.0009	0.2221	4.74	0	137.61
75	mdis11	1.0000	0.0014	1.0029	0.0009	0.2043	4.74	0	137.61
76	mdis12	1.0000	0.0014	1.0080	0.0008	0.1946	4.74	0	137.61
77	mdis13	1.0000	0.0014	0.9916	0.0009	0.1947	4.74	0	137.61
78	mdis14	1.0000	0.0014	0.9887	0.0008	0.2299	4.74	0	137.61
79	mdis15	1.0000	0.0014	0.9881	0.0010	0.2270	4.74	0	137.61
80	mdis16	1.0000	0.0014	1.0015	0.0008	0.1905	4.74	0	137.61
81	mdis17	1.0000	0.0014	0.9987	0.0008	0.1794	4.74	0	137.61
82	mdis18	1.0000	0.0014	0.9961	0.0008	0.1747	4.74	0	137.61
83	mdis19	1.0000	0.0014	0.9928	0.0009	0.1747	4.74	0	137.61
84	leuct022-02	1.0000	0.0046	1.0056	0.0013	0.2920	9.83	0	80.00
85	leuct022-03	1.0000	0.0036	1.0048	0.0013	0.1253	9.83	0	151.00
86	leuct024-01	1.0000	0.0054	0.9990	0.0015	1.0568	9.83	0	41.00
87	leuct024-02	1.0000	0.0040	1.0048	0.0014	0.1435	9.83	0	128.00
88	leuct025-01	1.0000	0.0041	0.9851	0.0014	0.4401	7.41	0	66.30
89	leuct025-02	1.0000	0.0044	0.9936	0.0013	0.2015	7.41	0	106.10
90	epri70b (PNL-31)	1.0009	0.0047	0.9995	0.0016	0.7631	-	688	146.15
91	epri70un (PNL-30)	1.0024	0.0060	0.9967	0.0015	0.5648	-	2	146.20
92	epri87b (PNL-33)	1.0024	0.0024	1.0046	0.0013	0.2780	-	1090	308.83
93	epri87un (PNL-32)	1.0042	0.0031	1.0034	0.0013	0.1894	-	1	308.99
94	epri99b (PNL-35)	1.0029	0.0027	1.0066	0.0009	0.1802	-	767	445.41
95	epri99un (PNL-34)	1.0038	0.0025	1.0088	0.0019	0.1353	-	2	445.57
96	saxtn104 (case 6)	1.0000	0.0023	1.0056	0.0017	0.1001	-	0	473.11
97	saxtn56b (case 3)	1.0000	0.0054	0.9980	0.0019	0.6523	-	337	95.24

No	Case name	Benchmark values		SCALE 4.4a Calculated Values		EALF (eV)	Enr wt% ^{235}U	B (ppm)	H/X
		k_{eff}	σ_{exp}	k_{eff}	σ_{calc}				
98	saxtn792 (case 5)	1.0049	0.0027	1.0027	0.0019	0.1547	-	0	249.70
99	saxton52 (case 1)	1.0028	0.0072	0.9987	0.0013	0.8878	-	0	73.86
100	saxton56 (case 2)	1.0019	0.0059	0.9997	0.0018	0.5450	-	0	95.29

In order to address situations in which the critical experiment being modeled was at other than a critical state (i.e., slightly super or subcritical), the calculated k_{eff} is normalized to the experimental k_{exp}, using the following formula (Eq.9 from Reference C.2):

$$k_{norm} = k_{calc} / k_{\exp}$$

In the following, the normalized values of the k_{eff} were used in the determination of the code bias and bias uncertainty.

C.5 **Trending Analysis**

The next step of the statistical methodology used to evaluate the code bias for the pool of experiments selected is to identify any trend in the bias. This is done by using the trending parameters presented in Table C.4.

Table C.4 Trending Parameters

Energy of the Average Lethargy causing Fission (EALF)
Fuel Enrichment (wt% ^{235}U)
Atom ratio of the moderator to fuel (H/X)
Soluble Boron Concentration

The first step in calculating the bias uncertainty limit is to apply regression–based methods to identify any trending of the calculated values of k_{eff} with the spectral and/or physical parameters. The trends show the results of systematic errors or bias inherent in the calculational method used to estimate criticality.

For the critical benchmark experiments that were slightly super or subcritical, an adjustment to the k_{eff} value calculated with SCALE 4.4a (k_{calc}) was done as suggested in Reference C.2. This adjustment is done by normalizing the calculated (k_{calc}) value to the experimental value (k_{exp}). This normalization does not affect the inherent bias in the calculation due to very small differences in k_{eff}. Unless otherwise mentioned, the normalized k_{eff} values (k_{norm}) have been used in all subsequent calculations.

Each subset of normalized k_{eff} values is first tested for trending against the spectral and/or physical parameters of interest (in this case, presented in Table C.4 above), using the built-in regression analysis tool from any general statistical software (e.g., Excel). Trending in this context is linear regression of unweighted calculated k_{eff} on the predictor variable(s) (spectral and/or physical parameters). In addition, the equations presented in Reference C.2 are also applied to check for a linear dependency in case of weighted k_{eff}, using as weight the factor $1/\sigma_t^2$ as previously discussed.

The linear regression fitted equation is in the form y(x) = a + bx, where y is the dependent variable (k_{eff}) and x is any of the predictor variables mentioned in Table C.4. The difference between the predicted y and actual value is known as the random error component (residuals).

The final validity of each linear trend is checked using well-established indicators or goodness-of-fit tests concerning the regression parameters. As a first indicator, the coefficient of determination (r^2) that is available as a result of using linear regression statistics, can be used to evaluate the linear trending. It represents the proportion of the sum of squares of deviations of the y values about their mean that can be attributed to a linear relation between y and x.

Another assessment of the adequacy of the linear model can be done by checking the goodness-of-fit against a null hypothesis on the slope (b) (Reference C.7, p. 371). The slope test requires calculating the test statistic "T" as in the following equation along with the corresponding statistical parameters (Reference C.7, p. 371).

$$T = \frac{\hat{\beta}_1}{s / \sqrt{S_{xx}}}$$

where, $\hat{\beta}_1$ is the estimated slope of the fitted linear regression equation,

$$S_{xx} = \sum_{i=1,n} (x_i - \bar{x})^2$$

and,

$$s = \frac{1}{(n-2)} \sum_{i=1,n} (y_i - \hat{y}_i)^2$$

where, $\hat{y}_i$ is the estimated value using the regression equation.

The test statistic is compared to the Student t-distribution ($t_{\alpha/2,n-2}$) with 95% confidence and n-2 degrees of freedom (Reference C.8, p.T-5), where n is the initial number of points in the subset. Given a null hypothesis H_0:β_1=0, of "no statistically significant trend exists (slope is zero)", the hypothesis would be rejected if $|T| > t_{\alpha/2,n-2}$. By only accepting linear trends that the data supports with 95% confidence, trends due to the randomness of the data are eliminated. A good indicator of this statistical process is evaluation of the P-value probability that gives a direct estimation of the probability of having linear trending due only to chance.

The last step of the regression analysis is determining whether or not the final requirements of the simple linear regression model are satisfied. The error components (residuals) need to be normally distributed with mean zero, and also the residuals need to show a random scatter

about the center line (no pattern). These requirements were verified for the present calculation by applying an omnibus normality test (Reference C.8, p.372) on the residuals.

The results of the trending parameter analysis for the criticality benchmark set (unweighted k_{eff}) are summarized in Table C.5.

Table C.5 Summary of Trending Analysis

Trend Parameter	n	Intercept	Slope	r^2	T	$t_{0.025,n-2}$	P-value	Goodness-of-fit Tests	Valid Trend
EALF	100	0.9937	0.002	0.061	2.53	1.987	0.013	Not Passed (residuals not normal and show a pattern –see Figure C.5)	No
Enrichment (wt% ^{235}U)	90[a]	0.9911	0.0008	0.070	2.57	1.991	0.012	Not passed (residuals not normal and show a pattern – see Figure C.6)	No
H/X	100	0.9952	-2.2E-06	0.001	-0.37	1.987	0.714	Not Passed	No
Boron in moderator (ppm)	100	0.9945	1.5E-06	0.009	0.95	1.987	0.345	Not passed	No

[a] Benchmark experiments with MOX fuel excluded.

The results in Table C.5 show that there are no statistically significant or valid trends of k_{eff} with the trending parameters. An additional check was done by checking if there are any trends on the weighted data. The results of the regression analysis obtained using weighted k_{eff} (with the weight factor $1/\sigma_t^2$ as previously discussed) show that the determination coefficient (r^2) has similar low values as in the above table, indicating very weak and statistically insignificant trends.

Figures C.1 to C.4 show the distribution of the normalized k_{eff} values versus the trending parameters investigated.

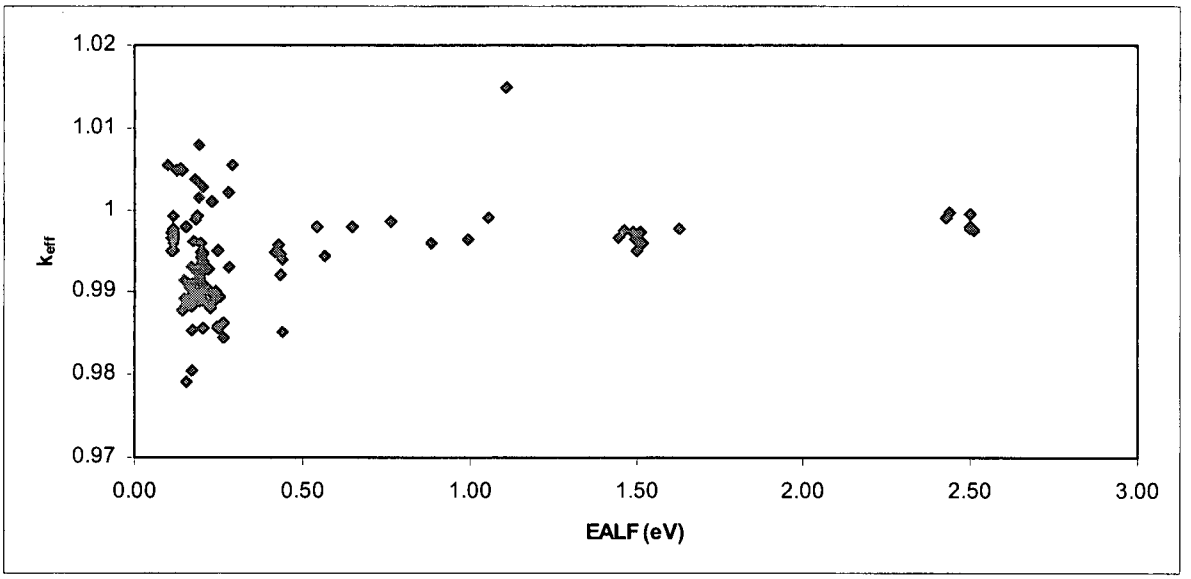

Figure C.1 Distribution of k_{eff} Data versus EALF for the Selected Pool of Benchmark Experiments

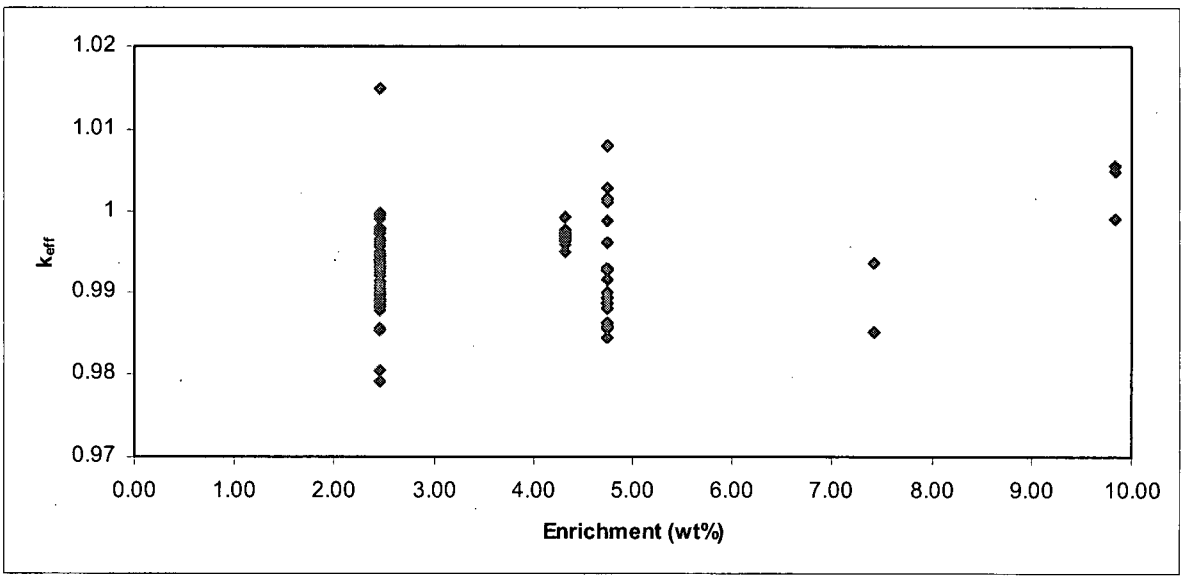

Figure C.2 Distribution of k_{eff} Data versus Enrichment (^{235}U) for the Selected Pool of Benchmark Experiments

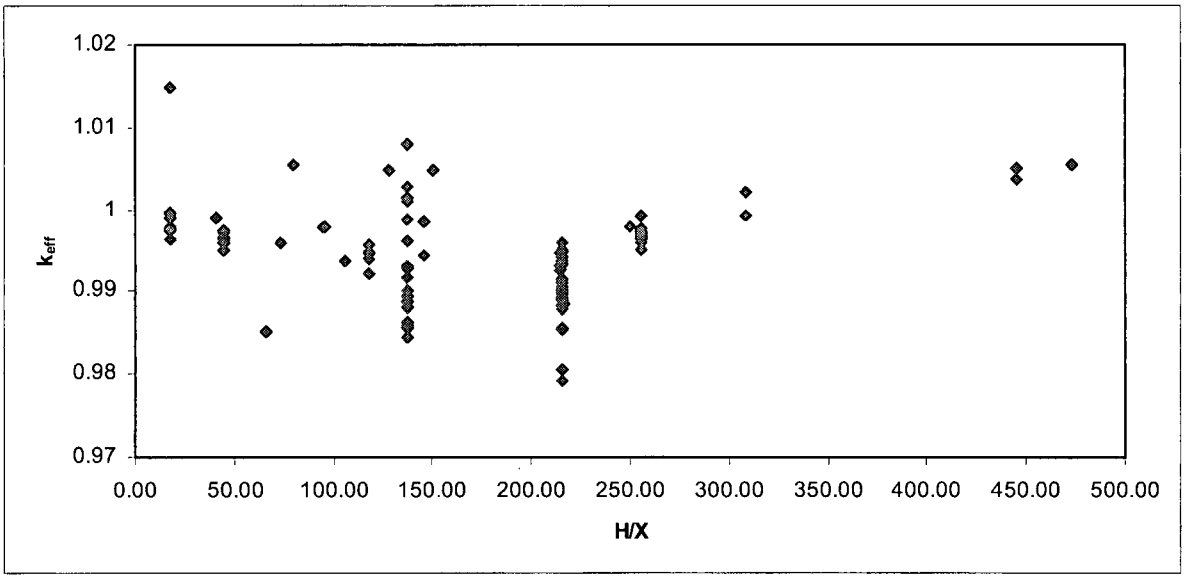

Figure C.3 Distribution of k_{eff} Data versus H/X for the Selected Pool of Benchmark Experiments

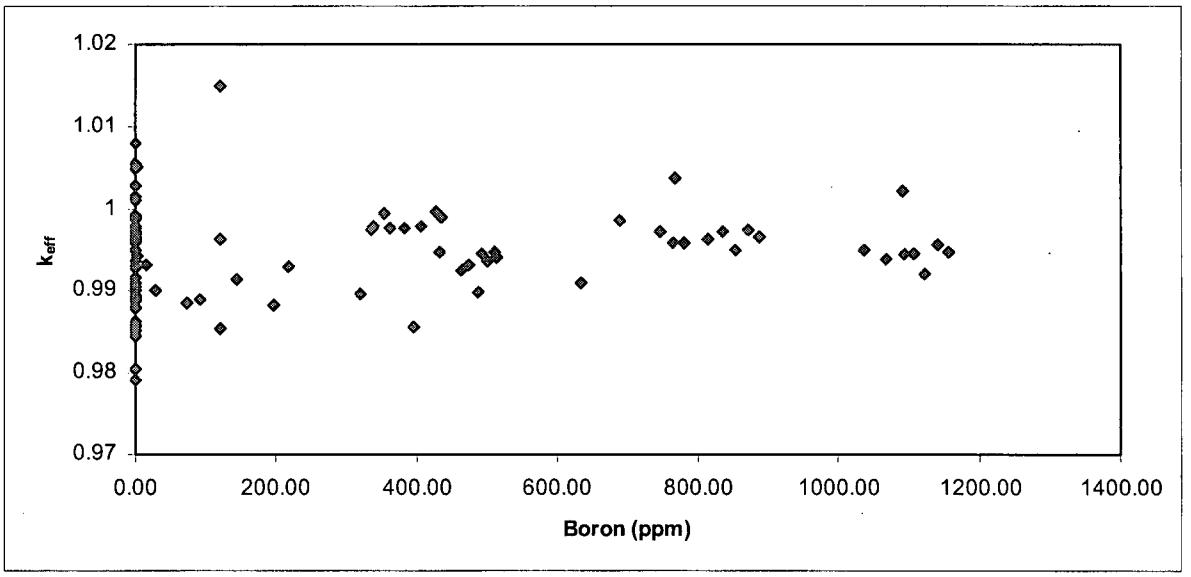

Figure C.4 Distribution of k_{eff} Data versus Soluble Boron Concentration for the Selected Pool of Benchmark Experiments

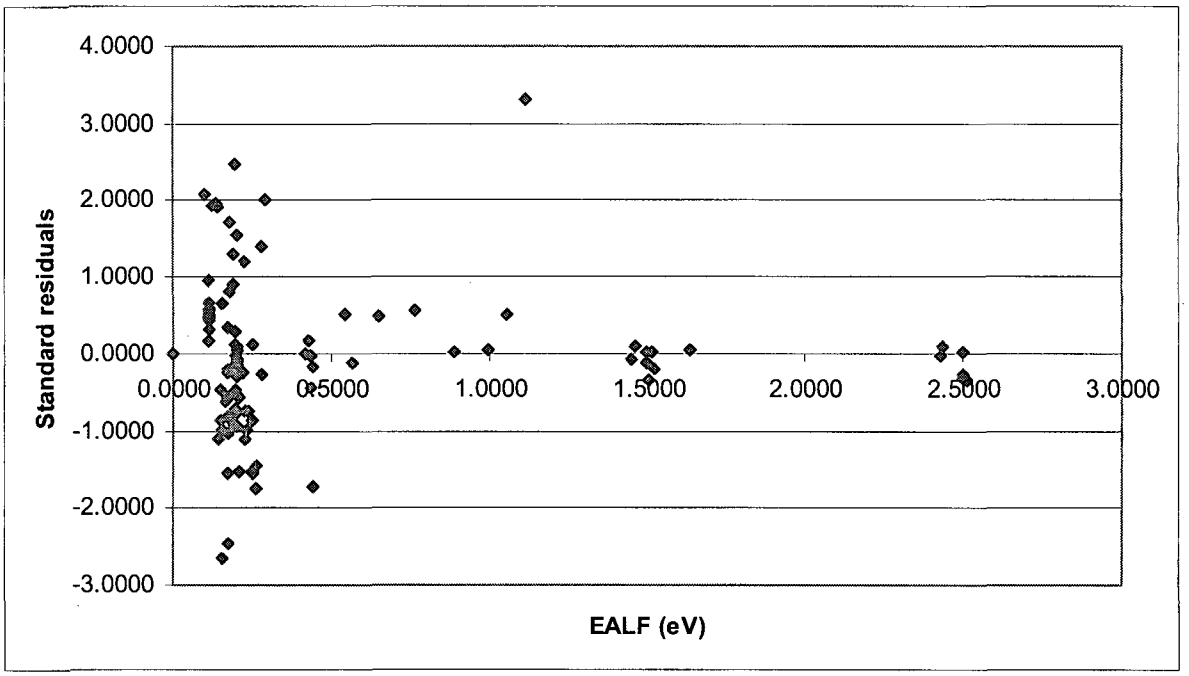

Figure C.5 Plot of Standard Residuals for Regression Analysis with EALF as Trending Parameter

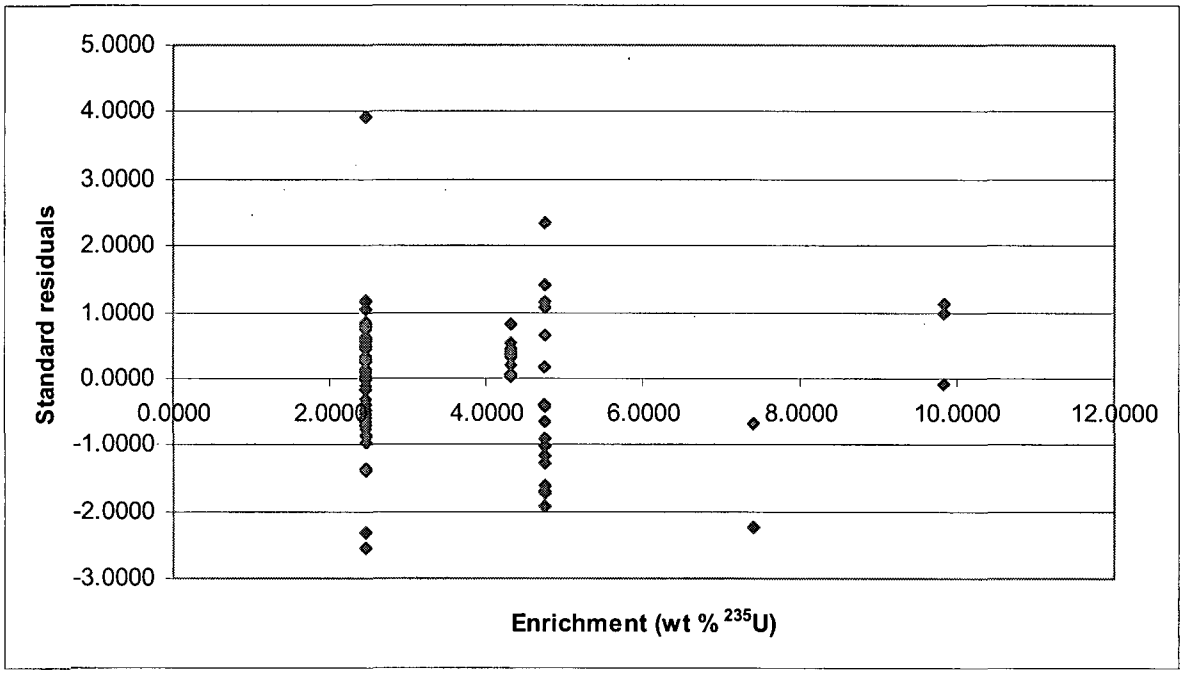

Figure C.6 Plot of Standard Residuals for Regression Analysis with Enrichment as Trending Parameter

C.6 Bias and Bias Uncertainty

For situations in which no significant trending in bias is identified, the statistical methodology presented in Reference C.2 suggests to first check the normality of the pool of k_{eff} data. Applying the Shapiro-Wilk test (Reference C.2) the null hypothesis of a normal distribution is not rejected. A visual inspection of the normal probability plot of the k_{eff} data shows that the pool of k_{eff} data for the selected benchmarks can be considered normally distributed.

This situation allows the application of the weighted single-sided lower tolerance limit to determine the bias uncertainty (Reference C.2). First by determining the factor for 95% probability at the 95% confidence level ($C_{95/95}$) and then multiplying it with the evaluated squared-root of the pooled variance, the uncertainty limit is determined.

From Reference C.9, $C_{95/95}$ for n equal to 100 is 1.927. The squared root of the pooled variance calculated using the formulas presented is:

$$s_P = \sqrt{s^2 + \overline{\sigma}^2} = (2.45212E\text{-}05+1.63005E\text{-}06)^{0.5} = 0.00511$$

Bias Uncertainty = $C_{95/95} * s_P$ = 1.927 * 0.00511 = 0.00985

The bias is obtained using the formula that includes the weighted average of k_{eff}

$$\text{Bias} = \overline{k}_{eff} - 1 = 0.99458 - 1 = -0.00542$$

These represent the final results which can be used to evaluate the maximum k_{eff} and $k_{95/95}$ values in the criticality analysis of the spent fuel pool. Note that this bias will be applied as a positive penalty in the equation for computation of $k_{95/95}$.

C.7 Area of Applicability

A brief description of the spectral and physical parameters characterizing the set of selected benchmark experiments is provided in Table C.6.

Table C.6 Range of Values of Key Parameters in Benchmark Experiments

Parameter	Range of Values
Geometrical shape	Heterogeneous lattices; Rectangular and hexagonal
Fuel type	UO_2 rods MOX fuel rods
Enrichment (for UO_2 fuel)	2.46 to 9.83 wt % ^{235}U
Lattice pitch	1.04 to 2.6416 cm
H/X	17.4 to 473
EALF	0.11 to 2.51 eV
Absorbers	Soluble boron Boron in plates:
Reflectors	Water Stainless Steel Aluminum

C.8 Bias Summary and Conclusions

This evaluation considers a selected set of criticality benchmark experiments with enrichments ranging from about 2.5 to about 10 wt% ^{235}U and includes some experiments with MOX fuel rods. The results of the evaluation provide the following information relative to the SCALE4.4a bias:

$$\text{Bias} = \bar{k}_{eff} - 1 = 0.99458 - 1 = -0.00542^*$$

Note that this bias will be applied as a positive penalty in the equation for computation of $k_{95/95}$:

$$\text{Bias Uncertainty} = C_{95/95}^* s_P = 1.927 * 0.00511^\dagger = 0.00985$$

The bias and its uncertainty (95/95 weighted single-sided tolerance limit) was obtained applying the appropriate steps of the statistical methodology presented in NUREG 6698 (Reference C.2) taking into account the possible trending of k_{eff} with various spectral and/or physical parameters.

---

* This will be applied as $bias_m = 0.00542$ in Section 6.6.

† s_P will be applied as $\sigma_m = 0.00511$ in Section 6.6. This is because the one sided tolerance multiplier is applied to the combined uncertainties in Section 6.6.

C.9 References

C.1 Nuclear Energy Agency, "International Handbook of Evaluated Criticality Safety Benchmark Experiments," NEA/NSC/DOC(95)03, Nuclear Energy Agency, Organization for Co-operation and Development, 2008.

C.2 Nuclear Regulatory Commission, "Guide for Validation of Nuclear Criticality Safety Calculational Methodology", NUREG/CR-6698, January 2001.

C.3 Bierman, S.R., Durst, B.M., Clayton, E.D., "Critical Separation Between Subcritical Clusters of 4.29 Wt% ^{235}U Rods in Water With Fixed Neutron Poisons," Battelle Pacific Northwest Laboratories, NUREG/CR-0073(PNL-2615).

C.4 Baldwin, M.N., et.al., "Critical Experiments Supporting Close Proximity Water Storage Of Power Reactor Fuel," BAW-1484-7, July 1979.

C.5 Hoovler, G.S., et.al., "Critical Experiments Supporting Underwater Storage of Tightly Packed Configurations of Spent Fuel Pins," BAW-1645-4, November 1981.

C.6 "Dissolution and Storage Experimental Program with $U(4.75)O_2$ Rods," Transactions of the American Nuclear Society, Vol. 33, pg. 362.

C.7 Rosenkrantz W.A., Introduction to Probability and Statistics for Scientists and Engineers, The McGraw-Hill, New York, NY, 1989.

C.8 D'Agostino, R.B. and Stephens, M.A., Goodness-of-fit Techniques. Statistics, Textbooks and Monographs, Volume 68, New York, New York, 1986.

C.9 Owen, D.B., Handbook of Statistical Tables, Addison-Wesley, Reading, MA.

Appendix D CASMO-4 Benchmarking for In-Rack Modeling

D.1 Introduction

The purpose of this Appendix is to provide qualification of the CASMO-4 code for use in the evaluation of the LaSalle Unit 2 Spent Fuel Pool with NETCO-SNAP-IN inserts. While the CASMO-4 code is not being used for the actual criticality calculation methodology, it is used for the selection of peak reactivity lattices and the determination of manufacturing uncertainties which have a depletion dependence. This evaluation is performed to address the guidance of References D.1 and D.2. The format and presentation follows the sample format presented in Section 6 of Reference D.2.

D.2 Code System

CASMO-4 is a multi-group, two-dimensional transport theory code with an in-rack geometry option where typical storage rack geometries can be defined on an infinite lattice basis. This code is used for fuel depletion and relative reactivity comparisons in a manner that is consistent with AREVA's NRC approved CASMO-4 / MICROBURN-B2 methodology (Reference D.3). The library files used in the evaluation are the standard CASMO-4 70 group library based on ENDFB-IV. The CASMO-4 computer code and data library are controlled by AREVA procedures and the version used in this analysis meets the requirements of Reference D.3. The CASMO-4 program is run on AREVA's HP-UX11 engineering workstations.

D.3 Benchmarking Methodology

Since the CASMO-4 code is a two-dimensional code that models the storage rack in an infinite array, it cannot be used to provide a stand-alone benchmark of finite criticality experiments. Consequently, the evaluation in this appendix takes a different approach – it provides a code to code comparison of the CASMO-4 code to the SCALE 4.4a KENO code. Benchmarking of the KENO code to criticality experiments was previously described in Appendix C.

The benchmarking of the CASMO-4 code in this Appendix is performed in two steps to demonstrate its acceptability for the two different ways that CASMO-4 is used in the LaSalle analysis.

- Identify the relative reactivity of a lattice with the use of the storage rack geometry option. This is addressed by determining the CASMO-4 uncertainty relative to KENO by comparison of calculated k-infinities from the two codes.
- Evaluate relative changes in reactivity associated with changes in manufacturing tolerances. For this evaluation, the differential k-infinities from the two codes are compared based upon the same input perturbations.

These different approaches are described in more detail in the following sections.

In addition to benchmarking against KENO, the CASMO-4 depletion uncertainty is established based on Reference D.3.

D.3.1 **CASMO-4 Uncertainty for Absolute k-infinite Relative to KENO**

The approach that is taken for the benchmarking of the in-rack CASMO-4 model is to perform a series of calculations with varied enrichments, geometries, and temperatures. The results of the CASMO-4 calculations are then compared to KENO results for the same configurations. The validation guidance of NUREG/CR-6698 (Reference D.2) is followed to determine a code uncertainty for CASMO-4 relative to KENO. The KENO calculations are treated as the critical experiments in the validation process. The validation includes ATRIUM-10 top and bottom lattices as well as ATRIUM-9 lattices.

D.3.2 **CASMO-4 Uncertainty for Δk-infinite Relative to KENO**

The capability of the CASMO-4 code to predict the change in reactivity associated with a perturbation of fuel parameters is demonstrated by comparison of Δk values obtained with KENO to those obtained with CASMO-4. The approach taken is to evaluate small perturbations in reactivity by varying the enrichment relative to a base case. The same cases used in the evaluation of the uncertainty of the absolute multiplication factor are used in this evaluation. The Δk values will be determined for both KENO and CASMO-4 for enrichment perturbations from the reference case.

The Δk values are compared between the two codes and a statistical evaluation similar to that identified in Reference D.2 is used to establish an uncertainty for the determination of Δk values with CASMO-4 relative to KENO.

D.3.3 **CASMO-4 Depletion Uncertainty**

The CASMO-4 depletion uncertainty is derived from the AREVA licensing topical report based on the extensive benchmarking that is documented within Reference D.3. Comparisons against critical experiments were performed by Studsvik with results reported in Table 2.1 of AREVA's CASMO-4/MICROBURN-B2 licensing topical report (Reference D.3). In addition, the beginning of cycle cold critical calculations reported in Table 2.2 of this same licensing topical report also provide comparisons to critical data. Results of these comparisons indicate that CASMO-4 results will have a standard deviation of [ ] Δk (Table 2.1 of Reference D.3) without depletion and a standard deviation of [ ] Δk (Table 2.2 of Reference D.3) when the majority of assemblies have been depleted*.

In addition to depletion effects, the [ ] Δk standard deviation from Reference D.3 also includes manufacturing and measurement uncertainties. Since it is difficult to separate these uncertainties, this entire value ([ ] Δk) will be used for the CASMO-4 depletion uncertainty when using the discrete void history levels from Reference D.3.

D.4 **Experiment Descriptions**

As noted, KENO calculations are used as the reference experiments. The evaluations are based on the LaSalle Unit 2 Spent Fuel Pool with NETCO-SNAP-IN inserts. The validation is performed using both bottom and top ATRIUM-10 and ATRIUM-9 lattice geometries within the LaSalle Unit 2 Spent Fuel Pool with NETCO-SNAP-IN inserts. Enrichment is varied in 0.05 increments above and below an assumed base enrichment level up to maximum delta of 0.25. The maximum peak reactivity of the fuel manufactured for LaSalle in the given geometry is represented within the range of enrichments evaluated. The calculations are reported for 4°C, 20°C and 100°C (277°K, 293°K and 373°K).

---

* The uncertainty of cold critical benchmarks effectively includes a depletion uncertainty since the majority of the bundles in the core are exposed. It is noted, that a cold in-sequence critical has significant similarities to an in-rack calculation since the majority of the control blades remain inserted effectively surrounding the majority of the fuel with a strong neutron absorber on two sides.

The minimum, base, and maximum enrichments for the ATRIUM-10 bottom (A10B), the ATRIUM-10 top (A10T) and the ATRIUM-9 (AT9) lattices are:

[

]

The fuel assembly data, rack geometry, and NETCO-SNAP-IN insert are the same as those for the LaSalle Unit 2 Spent Fuel Pool configuration.

D.5 Analysis of Validation Results

D.5.1 CASMO-4 Uncertainty for Absolute k-effective Relative to KENO

The calculated multiplication factors from KENO and CASMO were tabulated. The σ_{keno} terms are taken from each individual KENO calculation and the σ_{casmo} terms are set to the CASMO-4 convergence criteria for the individual case. (Use of the CASMO convergence is consistent with footnote 1 on page 6 of Reference D.2.) A combined uncertainty σ_{tot} was determined consistent with equation 3 of Reference D.2.

$$\sigma_{tot} = \sqrt{\sigma_{keno}^2 + \sigma_{casmo}^2}$$

The tabulated results are provided in Table D.1. The geometry is identified as either A10B (bottom lattice), A10T (top lattice), or AT9 (ATRIUM-9) along with the temperature and enrichment variations.

Table D.1 CASMO4 and KENO Validation Case Information

[

]

Table D.1 CASMO4 and KENO Validation Case Information *(Continued)*

[

]

Table D.1 CASMO4 and KENO Validation Case Information *(Continued)*

[

]

Since this is a comparison between two codes, the differences of the calculated values for the multiplication factor are determined. The results of the difference along with the components used in the statistical evaluation are provided in Table D.2.

Table D.2 CASMO - KENO Difference and Statistical Parameters

[

]

* Δk is $k_{CASMO} - k_{KENO}$

Table D.2 CASMO - KENO Difference and Statistical Parameters *(Continued)*

[

]

* Δk is $k_{CASMO} - k_{KENO}$

Table D.2 CASMO - KENO Difference and Statistical Parameters *(Continued)*

[

]

The weighted average difference (Δkbar), the variance about the mean s^2, and the average total uncertainty σ^2 are calculated using the weighting factor $1/\sigma_t^2$. The square root of the pooled variance is determined per Equation 7 of Reference D.2

* Δk is $k_{CASMO} - k_{KENO}$

$$S_p = \sqrt{s^2 + \sigma^2}$$

Weighted mean difference	Δkbar	[ ]	Ref D.2 Eq 6
Average total uncertainty	σ^2	[ ]	Ref D.2 Eq 5
Variance about mean	s^2	[ ]	Ref D.2 Eq 4
Square root of pooled variance	Sp	[ ]	Ref D.2 Eq 7

The CASMO-4 bias relative to KENO is [ ]. The bias uncertainty value is rounded up to [ ].

Normality test

Normality tests were performed on the combined data and the results were somewhat indeterminate but indicated potential non-normality. The data was then subdivided by temperature which is consistent with the use of CASMO-4 in comparing lattice results at the same temperature. In this comparison each temperature data set was determined to be a normal distribution. A single uncertainty for the combined data set is conservatively reported rather than individual temperature dependent uncertainty values.

Since this uncertainty value is only used to demonstrate that the CASMO-4 code can select the most reactive lattices for a given temperature, a 95/95 confidence multiplier is not determined.

Data Trending

No specific trending of the code bias was completed since CASMO-4 is not used directly for the determination of the absolute value of the multiplication factor. It is noted that the agreement is better at 4 °C than 100 °C.

Area of Applicability

The fuel and rack geometry as well as fuel enrichment were evaluated consistent with the LaSalle Unit 2 spent fuel pool. Therefore the area of applicability is specific to the LaSalle Unit 2 spent fuel pool with inserts.

D.5.2 **CASMO-4 Uncertainty for Δk-effective**

The actual KENO and CASMO calculations used in this evaluation are those used in Section D.5.1. In this evaluation, the relative reactivity change is evaluated by taking the delta with respect to the initial reference reactivity. A difference is then determined between the Δk values obtained with KENO and the Δk values obtained with CASMO-4 for the same perturbation.

Table D.3 Lattice Evaluations at 4°C

[

]

Table D.4 Lattice Evaluations at 20°C

[

]

Table D.5 Lattice Evaluations at 100°C

[

]

The average difference between the Δk values was [ ] with a standard deviation of [ ].

The Shapiro-Wilk data normality test and the Anderson-Darling goodness of fit for normality (see section 9.5.4.1 of Reference D.4) were performed on the Δk comparisons. Based on the test results and a visual inspection of the data, it is considered normally distributed.

For the data sample of 50 the single sided tolerance factor is 2.065 from Table 2.1 of Reference D.2. This is conservatively applied for 90 data samples.

Therefore, the 95/95 uncertainty is [ ].

Data Trending

A code bias is not used in the evaluation of incremental reactivity. Therefore, trending of the bias was not completed.

Area of Applicability

The fuel and rack geometry as well as fuel enrichment were evaluated consistent with the LaSalle Unit 2 spent fuel pool. Therefore the area of applicability is specific to the LaSalle Unit 2 spent fuel pool with inserts.

D.6 **Total CASMO-4 Uncertainty**

When applied on a differential basis a Δk predicted by CASMO-4 agrees with the KENO V.a based Δk with an uncertainty less than [ ] Δk, (see Section D.5). This can be combined with the [ ] Δk depletion uncertainty discussed in Section D.3.3 to obtain the total CASMO-4 uncertainty. A 95/95 uncertainty result is also obtained by multiplying these uncertainties by an appropriate multiplier. Since these values are independent they will be combined using the square root of the sum of the squares as shown in the following table. This process results in a total CASMO-4 uncertainty value of less than 0.007* Δk.

Uncertainty Value	σ	95/95 Multiplier	95/95 Uncertainty
Depletion	[ ]	2.0	[ ]
Calculational (Δk based)	[ ]	2.065	[ ]
Combined			[ ]

* An alternate approach for determining the reactivity worth of the uncertainty in the fuel depletion calculation is discussed in Section 5.A.5 of Reference D.1. "In the absence of any other determination of the depletion uncertainty, an uncertainty equal to 5% of the reactivity decrement to the burnup of interest is an acceptable assumption." While this section of Reference D.1 explicitly addresses analyses that credit reactivity depletion due to fuel burnup (i.e. burnup credit), recent discussions with the NRC indicate that 5% of the reactivity increment (BOL to peak reactivity) would be an acceptable representation of the depletion uncertainty to peak reactivity. Based on this information, 5% of the reactivity increment from BOL to peak reactivity was determined for the three reference bounding lattices. [

] Therefore, the uncertainty of a single assembly made up of these lattices will not differ significantly from the 0.007 Δk determined here.

D.7 Conclusions

A code bias uncertainty of [ ] was determined for CASMO-4 relative to KENO V.a in the determination of the absolute value of the multiplication factor. Based on this, it is demonstrated that the CASMO-4 code can be used for the characterization of the in-rack reactivity of fuel designs in the LaSalle Unit 2 spent fuel pool.

A standard deviation of [ ] was established for determining Δk with CASMO-4 relative to the Δk determined with KENO V.a. A 95/95 confidence multiplier of 2.065 is applicable for this uncertainty.

The evaluation of the ATRIUM-9, ATRIUM-10 bottom, and ATRIUM-10 top lattices demonstrated that there is no specific fuel geometry dependence relative to the use of CASMO-4 with respect to evaluating the in-rack reactivity.

The 0.01 Δk adder used when defining the REBOL lattices conservatively bounds the CASMO-4 uncertainty. Consequently, no CASMO bias or uncertainty is required in the final $k_{95/95}$ calculation.

D.8 References

D.1 Memorandum L. Kopp to T. Collins, "Guidance on the Regulatory Requirements for Criticality Analysis of Fuel Storage at Light-Water Reactor Power Plants," NRC, August 19, 1998. (NRC –ADAMS Accession Number ML072710248)

D.2 NUREG/CR-6698, "Guide for Validation of Nuclear Criticality Safety Calculational Methodology," USNRC, January 2001.

D.3 EMF-2158(P)(A) Revision 0, *Siemens Power Corporation Methodology for Boiling Water Reactors: Evaluation and Validation of CASMO-4/MICROBURN-B2,* Siemens Power Corporation, October 1999.

D.4 MIL-HDBK-5J, "Metallic Materials and Elements for Aerospace Vehicle Structures", Department of Defense, January 2003.

Distribution

Controlled Distribution

Richland

RJ DeMartino
RE Fowles
R Fundak
SW Jones
DP Jordheim
CD Manning
CM Powers
EE Riley
AW Will
PD Wimpy

ATTACHMENT 7
Summary of Regulatory Commitments

The following list identifies those actions committed to by Exelon Generation Company, LLC, (EGC) in this submittal. Any other actions discussed in the submittal represent intended or planned actions by EGC, are described only for information, and are not regulatory commitments.

COMMITMENT	COMMITTED DATE OR "OUTAGE"	COMMITMENT TYPE	
		ONE-TIME ACTION (YES/NO)	PROGRAM-MATIC (YES/NO)
The ATRIUM-10 fuel assembly design limitations will be incorporated in reload design documents and SFP criticality compliance procedures. Additionally, the design limitations will be reflected in Sections 9.1.2.1 and 9.1.2.2 of the LaSalle County Station (LSCS) Updated Final Safety Analysis Report (UFSAR).	Upon implementation of the proposed change	No	Yes
The Boraflex monitoring program will continue to be maintained for as long as EGC continues to credit Boraflex for criticality control, regardless of the implementation of NETCO-SNAP-IN® rack inserts.	Complete	No	Yes
The rack inserts will be installed in stages, with each stage of installation resulting in the use of a rack insert in all the spent fuel storage rack cells of a given individual spent fuel storage rack and all the cells of the first row and first column of adjoining spent fuel storage racks, such that all sides of the fuel assemblies within the spent fuel storage rack are adjacent to a face of the rack insert's wing.	Prior to crediting the neutron absorption capabilities of the NETCO-SNAP-IN® rack inserts for each individual Unit 2 spent fuel storage rack	Yes	No

ATTACHMENT 7
Summary of Regulatory Commitments

COMMITMENT	COMMITTED DATE OR "OUTAGE"	COMMITMENT TYPE	
		ONE-TIME ACTION (YES/NO)	PROGRAM-MATIC (YES/NO)
EGC will implement the Rio Tinto Alcan Composite Surveillance Program as described in Section 3.9 of Attachment 1 to ensure that the performance requirements of the Rio Tinto Alcan composite in the NETCO-SNAP-IN® rack inserts are met over the lifetime of the spent fuel storage racks with the rack inserts installed. A description of the program will be added to the LSCS UFSAR upon implementation of the proposed change.	Upon implementation of the proposed change	No	Yes